Inorg. Chem. **2002**, *41*, 2014–2025

Lithium Fluoroarylamidinates: Syntheses, Structures, and Reactions

Carsten Knapp, Enno Lork, Paul G. Watson, and RUdiger Mews*

Institut für Anorganische und Physikalische Chemie der Universität Bremen, Leobener Strasse NW2, D-28334 Bremen, Germany

Received October 22, 2001

Lithium fluoroarylamidinates $[(Ar_FC(NSiMe_3)_2Li)_n \cdot xD]$ (Ar_F = 4-$CF_3C_6H_4$, n = 2, D = OEt_2, x = 1 (**2a**); n = 1, D = TMEDA, x = 1 (**4a**); Ar_F = 2-FC_6H_4, n = 2, D = OEt_2, x = 1 (**2b**); Ar_F = 4-FC_6H_4, n = 2, D = OEt_2, x = 2 (**2c**); Ar_F = 2,6-$F_2C_6H_3$, n = 2, D = OEt_2, x = 1 (**2d**); n = 2, D = 2,6-$F_2C_6H_3CN$, x = 2 (**3d**); Ar_F = C_6F_5, n = 2, D = OEt_2, x = 1 (**2e**), n = 1, D = TMEDA, x = 1 (**4e**); n = 1, x = 2, D = OEt_2 (**5e**); D = THF (**6e**)) were prepared by the well-known method from $LiN(SiMe_3)_2$ and the corresponding nitrile in diethyl ether or by addition of the appropriate donor D to the respective diethyl ether complexes. Depending on the substituents at the aryl group and on the donors D, three different types of structures were confirmed by X-ray crystallography. Hydrolysis of **2e** gave $C_6F_5C(NSiMe_3)N(H)SiMe_3$ (**7e**) and $C_6F_5C(NH)N(H)SiMe_3$ (**8e**). The lithium fluoroarylamidinates **2a**–**2d** react with Me_3SiCl to give the corresponding tris(trimethylsilyl)fluoroarylamidines $Ar_FC(NSiMe_3)N(SiMe_3)_2$ (**9a**–**9d**). Attempts to prepare $C_6F_5C(NSiMe_3)N(SiMe_3)_2$ from **2e** and Me_3SiCl failed; however, the unprecedented cage $\{[C_6F_5C(NSiMe_3)_2Li]_4LiF\}$ (**10e**) in which a fluoride center is surrounded by a distorted trigonal bipyramid of five Li atoms was obtained from this reaction.

1. Introduction

Amidinates, $RC(NR')(NR'')^-$, especially arylbis(trimethylsilyl) derivatives, $ArC(NSiMe_3)_2^-$, are versatile ligands in the chemistry of main-group and transition metals and in lanthanide and actinide chemistry.[1] Their steric requirement corresponds to that of the Cp ligand,[2,3] and exchange of Cp^- by $ArC(NSiMe_3)_2^-$ reduces the electron density at the metal centers and modifies their activity in catalytic processes. For this reason attention has recently been turned to the arylbis(trimethylsilyl)amidinates, since the silyl groups decrease the donor ability; their reactivity can be influenced further by varying the aryl group, e.g., by introducing electron-withdrawing substituents. Particularly suitable for this purpose are fluorinated groups and fluorine itself. A few reports on (trifluoromethyl)aryl derivatives are found in the literature. The preparation of $[4\text{-}CF_3C_6H_4C(NSiMe_3)_2Li]$ has been reported;[4] $[2,4,6\text{-}(CF_3)_3C_6H_2C(NSiMe_3)_2]^-$ was introduced as a ligand into coordination chemistry by Edelmann and his group.[4] Contradictory reports are found in the literature for the existence of $[C_6F_5C(NSiMe_3)_2Li]$. Passmore et al. prepared the compound in situ from $LiN(SiMe_3)_2$ and C_6F_5CN and applied it successfully in the preparation of CNS heterocycles.[5] Eisen and co-workers isolated from the same starting materials in THF a 11:9 mixture of $[p\text{-}(Me_3Si)_2NC_6F_4CN]$ and $[p\text{-}LiN(C_6F_4CN)_2]$ in quantitative yield; both compounds were characterized by X-ray crystallography.[6] Teuben et al. obtained the expected amidinate $[C_6F_5C(NSiMe_3)_2Li]$ from diethyl ether.[7] They unequivocally characterized the compound as $[C_6F_5C(NSiMe_3)_2Li \cdot {}^1/_2OEt_2]$ by spectroscopic methods and elemental analysis and transferred the ligand to vanadium centers; e.g., $\{[C_6F_5C(NSiMe_3)_2]_2VClNCPh\}$ was characterized by X-ray crystallography.[7]

Since the importance of bis(trimethylsilyl)fluoroarylamidinates and tris(trimethylsilyl)amidines as reagents and ligands will increase, we began to investigate systematically their syntheses, structures, and reactions.

In the present paper we report on the preparation of $[4\text{-}CF_3C_6H_4C(NSiMe_3)_2Li]$, $[4\text{-}FC_6H_4C(NSiMe_3)_2Li]$, $[2\text{-}FC_6H_4C(NSiMe_3)_2Li]$, $[2,6\text{-}F_2C_6H_3C(NSiMe_3)_2Li]$, and $[C_6F_5C$-

* To whom correspondence should be addressed. Phone: 49-421-2183354. Fax: 49-421-218-4267. E-mail: mews@chemie.uni-bremen.de.

(1) For review: Edelmann, F. T. *Coord. Chem. Rev.* **1994**, *137*, 403−481.
(2) Recknagel, A.; Knösel, F.; Gornitzka, H.; Noltemeyer, M.; Edelmann, F. T. *J. Organomet. Chem.* **1991**, *417*, 363−375.
(3) Wedler, M.; Knösel, F.; Pieper, U.; Stalke, D.; Edelmann, F. T. *Chem. Ber.* **1992**, *125*, 2171−2181.
(4) Wedler, M.; Knösel, F.; Noltemeyer, M.; Edelmann, F. T. *J. Organomet. Chem.* **1990**, *388*, 21−45.
(5) Fairhurst, S. A.; Sutcliffe, L. H.; Preston, K. F.; Banister, A. J.; Partington, A. S.; Rawson, J. M.; Passmore, J. M.; Schriver, M. J. *Magn. Reson. Chem.* **1993**, *31*, 1027−1030.
(6) Shmulinson, M.; Pilz, A.; Eisen, M. S. *J. Chem. Soc., Dalton Trans.* **1997**, 2483−2486.
(7) Brussee, E. A. C.; Meetsma, A.; Hessen, B.; Teuben, J. H. *J. Chem. Soc., Chem. Commun.* **2000**, 497−498.

10.1021/ic011099t CCC: $22.00
Published on Web 03/28/2002

$(NSiMe_3)_2Li]$, complex formation of these compounds with different donors, and hydrolysis of the C_6F_5 derivative to give $C_6F_5C(NSiMe_3)N(H)SiMe_3$ (**7e**) and $C_6F_5C(NH)N(H)SiMe_3$ (**8e**). While the partially fluorinated lithium amidinates readily react with Me_3SiCl to give the corresponding $ArC(NSiMe_3)N(SiMe_3)_2$, attempts to prepare tris(trimethylsilyl)pentafluorophenylamidine, $C_6F_5C(NSiMe_3)N(SiMe_3)_2$, failed. The unprecedented cage $\{[C_6F_5C(NSiMe_3)_2Li]_4LiF\}$ (**10e**) was isolated in low yield from this reaction and characterized by X-ray crystallography.

2. Results and Discussion

2.1. Syntheses and Reactions of Amidinates and Amidines. Fluorine-containing lithium *N*,*N*′-bis(trimethylsilyl)benzamidinates are readily obtained by the addition of $LiN(SiMe_3)_2$ to the carbon center of benzonitriles,[4,8] followed by the migration of a silyl group.

$$2Ar_FC{\equiv}N + 2LiN(SiMe_3)_2 \xrightarrow{\text{diethyl ether}} \underset{\mathbf{2a-2e}}{\{[Ar_FC(NSiMe_3)_2Li]_2{\cdot}x OEt_2\}} \quad (1)$$

1a−**1e**

2a: $Ar_F = 4\text{-}CF_3C_6H_4$, $x = 1$
2b: $Ar_F = 2\text{-}FC_6H_4$, $x = 1$
2c: $Ar_F = 4\text{-}FC_6H_4$, $x = 2$
2d: $Ar_F = 2,6\text{-}F_2C_6H_3$, $x = 1$
2e: $Ar_F = C_6F_5$ $x = 1$

After removal of the solvent and of all volatile products in vacuo, the remaining dark tarry residues are recrystallized from hexane to give **2a**−**2e** as colorless or faint yellow solids in 50−70% yield.

2a was first reported by Oakley et al.[8] as an intermediate in the preparation of $4\text{-}CF_3C_6H_4C(NSiMe_3)N(SiMe_3)_2$. Edelmann et al. isolated solvent-free **2a**[4] by a procedure similar to ours. Prolonged pumping under vacuum might have led to a complete loss of the diethyl ether ligand. The controversial reports on **2e** were mentioned in the Introduction; our investigations fully confirm the results obtained by Teuben et al.[7] We also found that at low temperature in THF a completely different reaction pathway, described by Eisen et al.,[6] is followed.

With an excess of nitriles in reaction 1 the diethyl ether ligand is exchanged, e.g.

$$4(\mathbf{1d}) + 2LiN(SiMe_3)_2 \rightarrow \underset{\mathbf{3d}}{[2,6\text{-}F_2C_6H_3C(NSiMe_3)_2Li{\cdot}2,6\text{-}F_2C_6H_3CN]_2} \quad (2)$$

$$\mathbf{2a}, \mathbf{2e} + 2TMEDA \xrightarrow[\text{diethyl ether}]{\text{toluene}} 2[Ar_FC(NSiMe_3)_2Li{\cdot}TMEDA] \quad (3)$$

4a: $Ar_F = 4\text{-}CF_3C_6H_4$
4e: $Ar_F = 4\text{-}C_6F_5$

$$\mathbf{2e} + R_2O_{XS} \rightarrow 2[C_6F_5C(NSiMe_3)_2Li{\cdot}2R_2O] \quad (4)$$

5e: $R_2O = Et_2O$
6e: R_2O = THF

Exchange of diethyl ether and saturation of the coordination sphere of the Li centers followed by monomerization of **2** is achieved with TMEDA to give **4a** and **4e**. An excess of diethyl ether or THF will also cleave **2e** to give monomeric **5e** or **6e**, respectively.

Lithium benzamidinates are very sensitive to moisture; the reaction of **2e** with an equimolar amount of water gave the corresponding bis(trimethylsilyl)benzamidine **7e** in high yield.

$$\mathbf{2e} + 2H_2O \rightarrow \underset{\mathbf{7e}}{2C_6F_5C(NSiMe_3)N(H)SiMe_3} + 2LiOH + Et_2O \quad (5)$$

$$2(\mathbf{7e}) + H_2O \rightarrow \underset{\mathbf{8e}}{2C_6F_5C(NH)N(H)SiMe_3} + Me_3SiOSiMe_3 \quad (6)$$

The product of the second hydrolysis step, **8e**, was isolated in small amounts and also characterized by X-ray crystallography.

According to Oakley, the nucleophilicity of the amidinates is strongly reduced by electron-withdrawing substituents at the aryl ring; e.g., $[4\text{-}NO_2C_6H_4C(NSiMe_3)_2Li]$ does not react with Me_3SiCl to give the corresponding tris(trimethylsilyl)amidine even under very rigorous conditions.[8] While **2a**−**2d** readily react with Me_3SiCl to give the corresponding tris(trimethylsilyl)benzamidines **9a**−**9d** (**9a** was already reported by Oakley et al.[8]), we failed to prepare the pentafluorophenyl derivative **9e**.

$$\mathbf{2a-2d} + Me_3SiCl \rightarrow \underset{\mathbf{9a-9d}}{Ar_FC(NSiMe_3)N(SiMe_3)_2} + LiCl \quad (7)$$

From the reaction of **2e** with Me_3SiCl in toluene, a dark red oil was obtained; the ^{19}F NMR spectrum showed a large number of overlapping multiplets of different intensities in the aromatic region. Separation of the products of this mixture was not possible. From a solution of this oil in C_6D_6 after a few weeks, colorless crystals separated which were identified by X-ray crystallography as cage **10e**. In a first step of the formation of **10e** LiF is formed by decomposition of **2e**; LiF then acts as a template for the formation of cage **10e**. To date attempts to obtain single crystals of **10e** directly from **2e** and LiF have been unsuccessful.

2.2. Structure Investigations. 2.2.1. General Considerations. Only a few structures of lithium amidinates are reported in the literature, but these already show a remarkable diversity. Four principally different coordination modes of the amidinate ligands have been established (Scheme 1).

Transitions between these different types are fluid, and assignment to the different types is somewhat arbitrary, depending on the limits considered for LiN bond distances. The Li centers are normally four-coordinate, but here also, depending on the distances accepted as LiN bonds, three- or five-coordination can be discussed.

To date five different types have been structurally characterized: two different types of mononuclear complexes, $[RC(NR')(NR'')Li{\cdot}2D]$ (R = R′ = R″ = Ph; R = Ph, R′ =

(8) Boeré, R. T.; Oakley, R. T.; Reed, R. W. *J. Organomet. Chem.* **1987**, *331*, 161−167.

Scheme 1

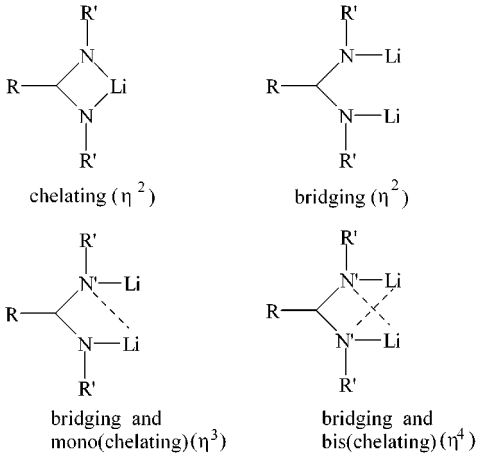

Scheme 2

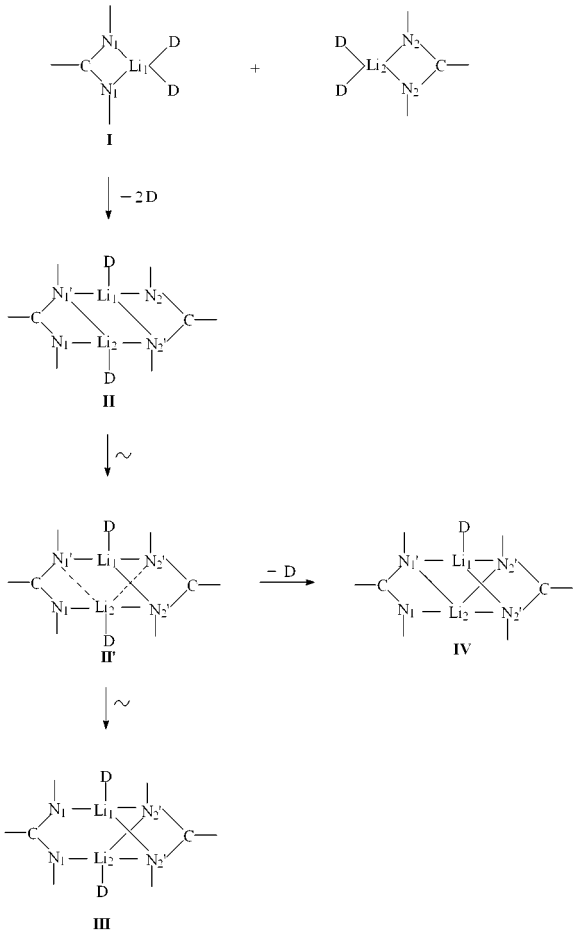

$SiMe_3$, R″ = myrtanyl; 2D = TMEDA)[9] (type **I**, Scheme 2) and [RC(NR′)(NR″)Li·3D] (R = R′ = R″ = Ph; 3D = NMe-$[(CH_2)_2NMe_2]_2$ (PMDETA));[10,11] three different types of dinuclear complexes, {$[RC(NR')(NR'')Li]_2$·2D} (R = 4-$CH_3C_6H_4$; R′ = R″ = $SiMe_3$; D = THF[12] (type **II**); R = R′ = R″ = Ph; D = $(Me_2N)_3PO$) (type **II**);[11] D = 4-$CH_3C_6H_4CN$ (type **III**);[13] R = ferrocenyl; R′ = R″ = cyclohexyl; D = OEt_2[14] (type **II**)) and the oxygen-bridged dimer $[RC(NR')(NR'')Li(\mu\text{-}(Me_2N)_3PO)_2LiRC(NR')(NR'')]$ (R = CH_3, R′ = R″ = Ph);[11] and two trinuclear complexes of similar structure, {$[RC(NR')(NR'')Li]_3D$} (R = C_6H_5, R′ = R″ = $SiMe_3$, D = C_6H_5CN;[15] R = 4-$CH_3C_6H_4$, R′ = R″ = $SiMe_3$, D = 4-$CH_3C_6H_4CN$[16]). Also the structurally characterized complex 4-$CH_3C_6H_4C(NSiMe_3)_2Li$·$Li(OEt_2)$-(4-$CH_3C_6H_4CN)N(SiMe_3)_2$[16] represents a precursor for the aforementioned dinuclear[13] and trinuclear[16] 4-$CH_3C_6H_4$ derivatives.

In our present investigation besides examples for complexes of type **I** (see Scheme 2) (**4a**, **4e**, **5e**, **6e**) (Figure 2) and type **III** (**3d**) (**2c** is regarded as type **II′**, the intermediate between type **II** and type **III**) (Figure 3) two new types of structures were confirmed: dinuclear complexes {$[RC(NR')(NR'')Li]_2D$} (**2a**, **2b**, **2d**, **2e**) (Figure 4) and the unprecedented fluoride-centered cage {$[C_6F_5C(NSiMe_3)_2Li]_4(LiF$} (**10e**) (Figure 5).

With the assumption that the Li centers are four-coordinate the structural relationships between the monomeric and the different dimeric complexes are best understood by starting from the monomeric complexes $[RC(NR')_2Li$·2D] (**I**), formed when strong donors D are present in excess (Scheme 2).

By loss of one donor molecule from each Li center the symmetric ladder-type[12] dimer **II** is formed with both ligands occupying three coordination sites (with N being monodentate, N′ bidentate). Rearrangement to the unsymmetrical "twisted" structure **III** with one bidentate and one tetradentate ligand occurs by cleaving bond N1′Li2 and forming bond

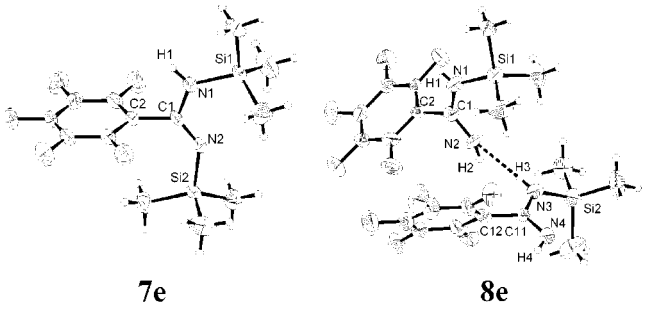

7e **8e**

Figure 1. Crystal structures and numbering scheme of **7e** and **8e**. The displacement ellipsoids are drawn at the 50% probability level. Selected bond lengths (pm) and angles (deg): (**7e**) C1−C2 153.1(5), C1−N1 137.0-(5), C1−N2 125.6(4), N1−Si1 175.883), N2−Si2 172.8 (3), N1−C1−N2 122.6(3), C2−C1−N1 112.5 (3), C2−C1−N2 124.8(3), C1−N1−Si1 125.6-(3), 135.4 (3); (**8e**) C1−C2 149.6 (10), C1−N1 138.0(9), C1−N2 126.3-(9), N1−Si1 175.8(7), N1−C1−N2 121.1(7), C2−C1−N1 115.6(3), C2−C1−N2 123.3(6), C1−N1−Si1 125.0(5), 147.7(11), C11−N3 136.9(10), C11−N4 127.4(10), N3−Si2 174.8(8), N3−C11−N4 119.3(7), C12−C11−N3 116.6(7), C12−C11−N4 124.0(7), C11−N3−Si2 126.4(6).

(9) Averbuj, C.; Tish, E.; Eisen, M. S. *J. Am. Chem. Soc*. **1998**, *120*, 8640−8646.
(10) Cragg-Hine, I.; Davidson, M. G.; Mair, F. S.; Raithby, P. R.; Snaith, R. *J. Chem. Soc., Dalton Trans.* **1993**, 2423−2424.
(11) Barker, J.; Barr, D.; Barnett, N. D. R.; Clegg, W.; Cragg-Hine, I.; Davidson, M. G.; Davies, R. P.; Hogdson, S. M.; Howard, J. A. K.; Kilner, M.; Lehmann, C. W.; Lopez-Solera, I.; Mulvey, R. E.; Raithby, P. R.; Snaith, R. *J. Chem. Soc., Dalton Trans.* **1997**, 951−955.
(12) Stalke, D.; Wedler, M.; Edelmann, F. *J Organomet. Chem*. **1992**, *431*, C1−C5.
(13) Eisen, M. S.; Kapon, M. *J. Chem. Soc., Dalton Trans.* **1994**, 3507−3510.
(14) Hagadorn, J. R.; Arnold, J. A. *Inorg. Chem*. **1997**, *36*, 132−133.
(15) Gebauer, T.; Dehnicke, K.; Goesmann, H.; Fenske, D. *Z. Naturforsch*. **1994**, *49b*, 1444−1447.
(16) Lisovskii, A.; Botoshanskii, M.; Eisen, M. *J. Chem. Soc., Dalton Trans.* **2001**, 1692−1698.

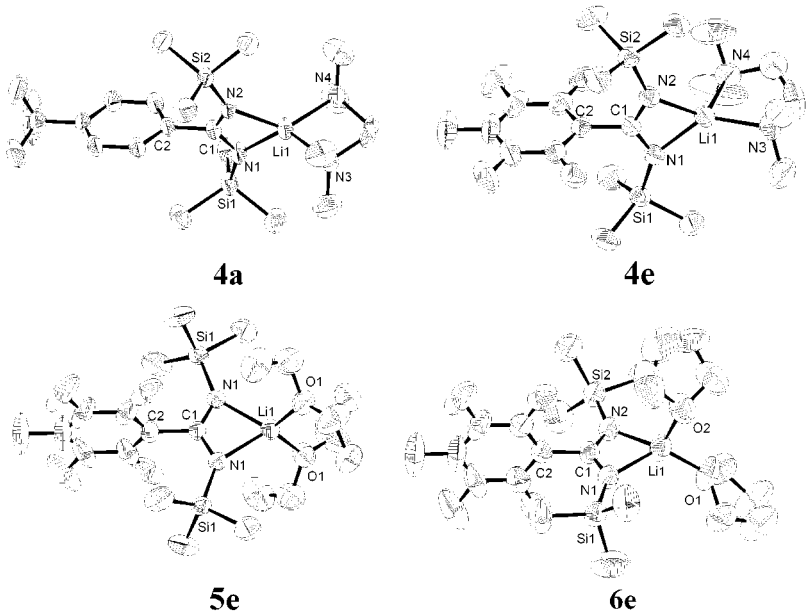

Figure 2. Crystal structures and numbering scheme of **4a**, **4e**, **5e**, and **6e**. The displacement ellipsoids are drawn at the 50% probability level, and the hydrogen atoms have been omitted for clarity. Selected bond lengths (pm) and angles (deg): (**4a**) C1−C2 150.8(3), C1−N1 132.6(3), C1−N2 132.5(3), N1−Si1 170.6(2), N2−Si2 170.21(19), N1−Li1 201.9(4), N2−Li1 201.6(4), N3−Li1 208.6(4), N4−Li1 209.7(4), N1−C1−N2 120.72(19); (**4e**) C1−C2 153.0(4), C1−N1 131.0(4), C1−N2 132.0(4), N1−Si1 171.6(2), N2−Si2 171.1(3), N1−Li1 202.0(5), N2−Li1 202.5(6), N3−Li1 210.0(6), N4−Li1 210.0(6), N1−C1−N2 122.1(3); (**5e**) C1−C2 152.7(5), C1−N1 131.5(2), N1−Si1 171.2(2), N1−Li1 206.3(5), O1−Li1 195.3(4), N1−C1−N2 122.6(3); (**6e**) C1−C2 153.5(6), C1−N1 131.1(5), C1−N2 129.9(5), N1−Si1 169.5(4), N2−Si2 169.9(4), N1−Li1 204.4(9), N2−Li1 204.0(9), O1−Li1 192.0(9), O2−Li1 193.6(11), N1−C1−N2 122.5(4).

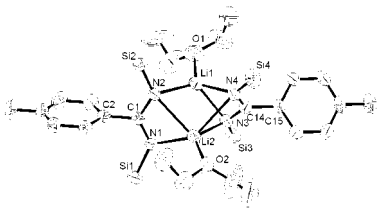

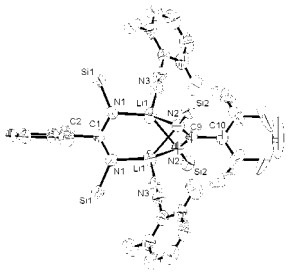

Figure 3. Crystal structures and numbering scheme of **2c** and **3d**. The displacement ellipsoids are drawn at the 50% probability level. The hydrogen atoms and methyl groups at the silicon atoms have been omitted for clarity. Selected bond lengths (pm) and angles (deg): (**2c**) C1−C2 151.1(4), C1−N1 131.2(3), C1−N2 134.5(3), N1−Si1 173.2(2), N2−Si2 172.9(2), N1−Li2 201.6(6), N2−Li1 205.8(6), N2−Li2 259.4(6), C14−C15 151.5(4), C14−N3 133.4(4), C14−N4 131.6(4), N3−Si3 172.6(2), N4−Si4 172.5(3), N3−Li1 223.7(6), N3−Li2 212.6(6), N4−Li1 211.9(6), N4−Li2 269.5(6), N1−C1−N2 121.7(2), N3−C14−N4 119.4(3), Li1−Li2 247.9(7), Li1−O1 197.4(6), Li2−O2 197.8(6); (**3d**) C1−C2 152.5(6), C1−N1 132.4(3), N1−Si1 172.3(3), Ni−Li1 200.9(6), C9−C10 150.4(6), C9−N2 132.1(3), N2−Si2 172.9(3), N2−Li1 216.1(6), N1−C1−N1 123.5(4), N2−C9−N2 118.8(4), Li1−Li1 244.1(11), Li1−O1 209.4(6).

N2Li2 (giving N2′Li2). Type **IV** with the composition {[RC(NR′)$_2$Li]$_2$D} results from **II** from the loss of a further D from Li2; the empty coordination site at Li2 is filled by the former N2.

The ladder-type structure **II** consists of three four-membered heterocycles; a central Li_2N_2 ring is connected to two CN_2Li systems. The cagelike structure **III** consists of two six-membered CN_3Li_2 heterocycles and one four-membered N_2Li_2 ring bridged by a CR′ group. In **IV** the center of five interconnected four-membered rings is formed by two Li_2N_2 units completed by three LiN_2C ring systems.

Our investigations show that the proposed structure types are idealized; experimental results deviate more or less from **II**−**IV**. Compound **2c** shows a structure similar to that of the intermediate type **II**′. Type **III** is verified in compound **3d**; this type was already described for the phenyl derivative (R = 4-$CH_3C_6H_4$, R′ = R″ = Me_3Si, D = 4-$CH_3C_6H_4CN$).[13] For this arrangement "slim" ligands, e.g., nitriles RCN, are necessary, which do not interfere sterically with the substituents R′.

2a, **2b**, **2d**, and **2e** with only one donor ligand D belong to type **IV**.

2.2.2. X-ray Structures of Pentafluorophenyl-*N,N*′- bis-(trimethylsilyl)amidine) (7e) and Pentafluorophenyl(trimethylsilyl)amidine) (8e).

From the hydrolysis of [$C_6F_5C(NSiMe_3)_2Li$] the amidines $C_6F_5C(NSiMe_3)N(H)SiMe_3$ (**7e**) and $C_6F_5C(NH)N(H)SiMe_3$ (**8e**) were obtained. They might be considered as "the most simple amidinate complexes where a proton is coordinated by an amidinate". X-ray structure determinations of silylated amidines $RC(NSiMe_3)N(SiMe_3)_2$, $RC(NSiMe_3)N(H)SiMe_3$, or $RC(NH)N(H)SiMe_3$ are rare; to date only that of PhC(NSiMe$_3$)N(SiMe$_3$)$_2$ has been reported,[17] but X-ray structures

(17) Ergezinger, C.; Weller, F.; Dehnicke, K. *Z. Naturforsch.* **1988**, *43b*, 1119−1124.

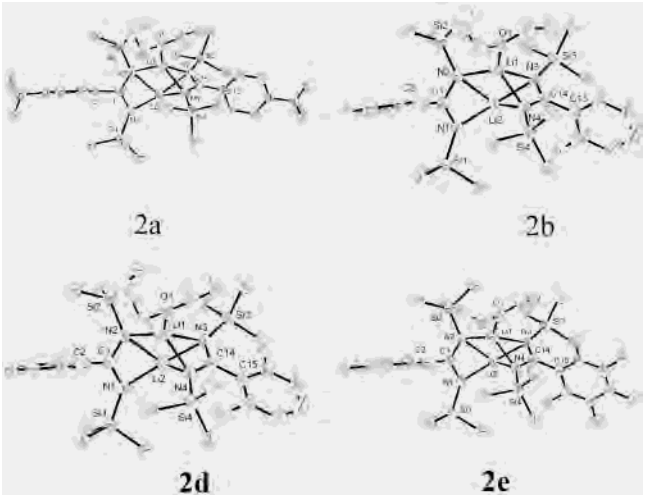

Figure 4. Crystal structures and numbering scheme of **2a**, **2b**, **2d**, and **2e**. The displacement ellipsoids are drawn at the 50% probability level. The hydrogen atoms have been omitted for clarity. Selected bond lengths (pm) and angles (deg): (**2a**) C1−C2 151.3(4), C1−N1 131.4(3), C1−N2 135.3(4), N1−Si1 173.5(3), N2−Si2 173.6(2), N1−Li2 203.0(6), N2−Li1 211.0(7), N2−Li2 220.3(6), C14−C15 151.3(4), C14−N3 132.9(4), C14−N4 132.6(4), N3−Si3 173.4(3), N4−Si4 172.9(6), N3−Li1 240.8(7), N3−Li2 218.3(6), N4−Li1 212.8(6), N4−Li2 217.4(6), N1−C1−N2 121.0(3), N3−C14−N4 118.3(6), Li1−Li2 231.5(8), Li1−O1 195.2(6); (**2b**) C1−C2 151.3(5), C1−N1 132.0(5), C1−N2 133.9(5), N1−Si1 172.3(3), N2−Si2 173.4(3), N1−Li2 197.8(8), N2−Li1 213.1(8), N2−Li2 216.4(9), C14−C15 151.1(6), C14−N3 132.5(5), C14−N4 131.8(5), N3−Si3 172.5(3), N4−Si4 173.8(3), N3−Li1 245.3(10), N3−Li2 207.0(8), N4−Li1 205.7(8), N4−Li2 228.3(10), N1−C1−N2 121.1(3), N3−C14−N4 119.5(4), Li1−Li2 235.7(12), Li1−O1 195.8(9); (**2d**) C1−C2 151.8(3), C1−N1 130.5(3), C1−N2 135.0(3), N1−Si1 172.67(17), N2−Si2 172.91(18), N1−Li2 199.8(4), N2−Li1 212.8(5), N2−Li2 214.1(5), C14−C15 151.2(3), C14−N3 132.4(3), C14−N4 131.6(3), N3−Si3 172.89(18), N4−Si4 173.41(18), N3−Li1 244.8(6), N3−Li2 205.4(4), N4−Li1 206.1(5), N4−Li2 236.9(5), N1−C1−N2 121.97(18), N3−C14−N4 120.10(18), Li1−Li2 236.3(6), Li1−O1 195.9(5); (**2e**) C1−C2 152.0(3), C1−N1 129.9(3), C1−N2 134.3(3), N1−Si1 173.45(19), N2−Si2 173.3(2), N1−Li2 200.(5), N2−Li1 211.3(5), N2−Li2 214.9(5), C14−C15 152.0(3), C14−N3 132.3(3), C14−N4 131.9(3), N3−Si3 172.65(19), N4−Si4 174.2(2), N3−Li1 255.4(6), N3−Li2 203.7(5), N4−Li1 205.8(5), N4−Li2 237.2(6), N1−C1−N2 122.5(2), N3−C14−N4 120.9(2), Li1−Li2 238.8(7), Li1−O1 193.5(5).

of the related amidines PhC(NPh)(NHPh)[18] and PhC(NH)-(NH_2)[19] have been described.

Details of the structure determinations of **7e** and **8e** are given in Table 4; the molecular structures are shown in Figure 1. Investigations on **7e** show that the proton in the amidine group $-C(=NSiMe_3)(-N(H)SiMe_3)$ is in an *E*-position; the amidinate group is not chelating the proton. Since no hydrogen bridging between N1 and N2 is observed, the distances CN1 (137.0(5) pm) and CN2 (125.6(4) pm) show distinct single and double bond character. The average of these two distances (131.3 pm) is exactly the same as that found for chelating (η^2) $C_6F_5C(NSiMe_3)_2^-$ in Li complexes (vide infra). The Si2N2 bond to the sp^2-hybridized nitrogen (172.8(2) pm) is significantly shorter than Si1N1 (175.8(3)), where the Me_3Si group is attached to an sp^3 nitrogen. The smallest angle at the exactly planar C1 is C2C1N1 (112.5(3)°); this is not due to hydrogen bonding between N1 and the fluorine at C3 of the C_6F_5 ring (d_{H-F} = 311 pm). The N1C1N2 angle of 122.6(3)° does not change when the amidinate ligand acts η^2-chelating toward Li centers (section 2.2.3). As also found in the lithium complexes, with 84.1(8)°, the torsion angle τ between the planes of the pentafluorophenyl ring and the NCN group is close to 90°.

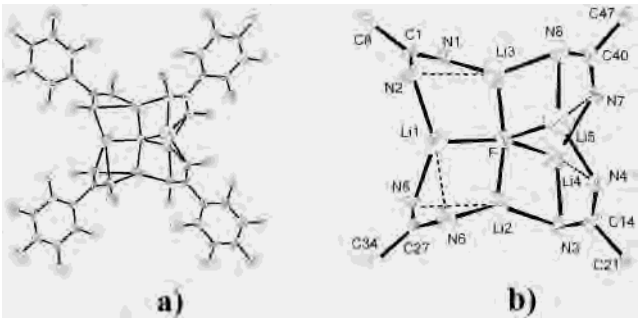

Figure 5. (a) Crystal structure of **10e**. The displacement ellipsoids are drawn at the 50% probability level, and the methyl groups have been omitted for clarity. (b) Part of the Li−F cage of **10e** showing the interaction of the fluorine center with the macrocyclic cryptand. Full lines represent bonds in the macrocyclic cryptand and to the fluorine atom, dashed lines weak Li−N transannular interactions. Selected bond lengths (pm) and angles (deg): F−Li1 197(2), F−Li(2) 187.9(19), F−Li3 189(2), F−Li4 190(2), F−Li5 194(2), C1−C8 155.6(13), C1−N1 132.2(12), C1−N2 133.2 (12), N1−Li3 199(2), N2−Li1 208(2), N2−Li3 258(2), C14−C21 153.3(13), C14−N3 130.1(13), C14−N4 131.6 (13), N3−Li2 213.4(19), N3−Li4 205-(2), N4−Li4 264(3), N4−Li5 205(2), C27−C34 154.0(13), C27−N5 131.1-(12), C27−N6 132.2(12), N5−Li1 200(2), N5−Li2 249.0(19), N6−Li1 269(2), N6−Li2 199.2(19), C40−C47 152.1(13), C40−N7 131.3(12), C40−N8 133.6(12), N7−Li4 208(2), N7−Li5 271(3), N8−Li3 205(2), N8−Li5 208(3), Li2−F−Li3 167.0(9), Li1−F−Li4 144.4(11), Li1−F−Li5 138.9-(11), Li4−F−Li5 76.5(10), Li2−F−Li4 144.4(11), Li1−F−Li2 80.6(8), Li1−F−Li3 86.5(3), Li2−F−Li4 87.2(9), Li2−F−Li5 103.9(9), Li3−F−Li4 102.7(10), Li3−F−Li5 86.8(10).

In the second hydrolysis step a Me_3Si group is lost from N2; according to our structure investigations **8e** is $C_6F_5C(NH)N(H)SiMe_3$ and not $C_6F_5C(NSiMe_3)NH_2$. Some small changes in the geometry of the amidine group result from this exchange of a further Me_3Si group by a proton. Compared to **7e** the C=N bond distance in the imino group slightly increases to 127.1 pm, the C−N bond length of the amino group is not affected, and the C−C bond to the aryl group is significantly shorter (148.7 pm compared to 153.1(5) pm in **7e**). The NCN angle in **8e** (120.2°) is 2.4° smaller than that in **7e**. This is not necessarily due to steric reasons, because this angle is 121.5° in PhC(NHPh)(NPh)[18] and 124.4° in PhC(NH)(NH_2).[19] Comparing **7e** and **8e**, the differences in the bond distances, in the bond and torsion angles (τ decreases in **8e** to 62.8(6)° and 63.8(5)° in the two independent molecules) might be a consequence of hydrogen bonding between H3 of the amino group and N2 of the imino group of a neighboring molecule.

2.2.3. X-ray Structures of Mononuclear Lithium Amidinate Complexes [ArC(NSiMe$_3$)$_2$Li·2D]. In the presence of an excess of strong donor ligands mononuclear lithium amidinate complexes are formed. Details of the structure determination of [4-$CF_3C_6H_4C(NSiMe_3)_2Li$·TMEDA] (**4a**), [$C_6F_5C(NSiMe_3)_2Li$(TMEDA] (**4e**), [$C_6F_5C(NSiMe_3)_2Li$·$2OEt_2$] (**5e**), and [$C_6F_5C(NSiMe_3)_2Li$·2THF] (**6e**) are given in Table 3; Figure 2 shows the structures of the compounds. A common feature of all structures is a central four-membered CN_2Li ring; a slight deviation from planarity is

(18) Alcock, N. W.; Barker, J.; Kilner, M. *Acta Crystallogr*. **1988**, *C44*, 712−715.
(19) Barker, J.; Philips, P. R.; Wallbridge, M. G. H.; Powell, H. R. *Acta Crystallogr*. **1996**, *C52*, 2617−2619.

Table 1. Crystal Data and Structure Refinement for **2a**, **2b**, **2d**, and **2e**[a]

	2a	**2b**	**2d**	**2e**
empirical formula	$C_{32}H_{54}F_6Li_2N_4OSi_4$	$C_{30}H_{54}F_2Li_2N_4OSi_4$	$C_{30}H_{52}F_4Li_2N_4OSi_4$	$C_{30}H_{46}F_{10}Li_2N_4OSi_4$
fw	751.03	651.01	687.00	794.95
T/K	173(2)	173(2)K	173(2)	173(2)
λ/Å	0.71073	0.71073	0.71073	0.71073
cryst syst	monoclinic	monoclinic	monoclinic	monoclinic
space group	$P2_1/n$	$P2_1/n$	$P2_1/n$	$P2_1/n$
a/Å	16.362(15)	11.1340(10)	11.045(2)	11.040 (1)
b/Å	11.402(2)	16.8500(10)	16.849(2)	17.153(1)
c/Å	23.046(3)	20.522(2)	20.880(7)	21.349(2)
α/deg	90	90	90	90
β/deg	103.15(3)	92.920(10)	93.03(2)	90.63(1)
γ/deg	90	90	90	90
V/Å^3	4190 (10)	3845.1 (6)	3880.3(15)	4042.6(6)
Z	4	4	4	4
ρ_{calcd}/g cm^{-3}	1.192	1.125	1.176	1.306
μ(Mo Kα)/mm^{-1}	0.197	0.191	0.200	0.222
R1, wR2 [$I > 2\sigma(I)$]	0.0533, 0.1257	0.0710, 0.1830	0.0489, 0.1201	0.0510, 0.1257
R1, wR2 (all data)	0.0850, 0.1377	0.1184, 0.2053	0.0778, 0.1363	0.0790, 0.1425

[a] Details in common: Refinement method full-matrix least-squares on F^2; $\omega-2\theta$ scans; Siemens P4 diffractometer; $R1 = \sum||F_o| - |F_c||/\sum|F_o|$; $wR2 = \{\sum[w(F_o^2 - F_c^2)^2/\sum[w(F_o^2)^2]\}^{1/2}$; programs SHELX-97[29] and DIAMOND.[30]

Table 2. Crystal Data and Structure for **2c** and **2d**[a]

	2c	**3d**
empirical formula	$C_{34}H_{64}F_2Li_2N_4O_2Si_4$	$C_{40}H_{48}F_8Li_2N_6Si_4$
fw	725.13	891.08
T/K	173(2) K	173(2)
λ/Å	0.71073	0.71073
cryst syst	monoclinic	monoclinic
space group	$P2_1/n$	$C2/c$
a/Å	10.686(2)	19.282(4)
b/Å	17.016(4)	18.171(4)
c/Å	24.506(4)	14.203(3)
α/deg	90	90
β/deg	92.550(10)	105.87(3)
γ/deg	90	90
V/Å^3	4451.6(15)	4786.7(18)
Z	4	4
ρ_{calcd}/g cm^{-3}	1.082	1.236
μ(Mo Kα)/mm^{-1}	0.173	0.189
R1, wR2 [$I > 2\sigma(I)$]	0.0652, 0.1543	0.0509, 0.1048
R1, wR2 (all data)	0.1169, 0.1834	0.1074, 0.1169

[a] Details in common: Refinement method full-matrix least-squares on F^2; $\omega-2\theta$ scans; Siemens P4 diffractometer; $R1 = \sum||F_o| - |F_c||/\sum|F_o|$; $wR2 = \{\sum[w(F_o^2 - F_c^2)^2/\sum[w(F_o^2)^2]\}^{1/2}$; programs SHELX-97[29] and DIAMOND.[30]

only observed for **4e** (sum of the angles 358.9°). In all compounds the CNLi angles at the nitrogens differ only slightly (83.7−84.7°); the NLiN angles (68.0−69.6°) are a little influenced by the NCN angles, which are dependent upon the substituents at the aryl groups. In **4a** this angle is slightly smaller (120.7(2)°) than in the C_6F_5 derivatives **4e** (122.1(3)°), **5e** (122.6(3)°), and **6e** (122.5(4)°). The average CN bond distances in the amidinate group of **4e**−**6e** are 131.5−130.3 pm; for **4a** an average distance of 132.5 pm was determined. The torsion angle τ of the phenyl groups relative to the plane of the C1N1Li1N2 is close to 90°.

From the present data the influences of the different substituents at the amidinate group RC(NR′)(NR″) on the bonding situation at the lithium center can only be tentatively discussed. Comparison of **4a** and **4e** with [PhC(NPh)$_2$Li·TMEDA][19] suggests as a general trend that variation of the substituents has almost no influence on the LiN bond distances. Introducing silyl groups at the nitrogen and electron-withdrawing groups at the aryl ring slightly decreases the average CN distances, decreases the CNLi angles, and increases the NCN angle. The "bite" angle NLiN increases when Me_3Si groups are introduced at the nitrogens; variations within the aryl group have almost no influence.

Comparison of **4a** and **4e** with **5e** and **6e** shows that the exchange of the coligands has a greater influence on the bonding situation at the central Li than variations in the aryl group of the amidinate ligand. By substituting the TMEDA ligand of **4e** by oxygen donors, by diethyl ether in **5e**, or by THF in **6e**, the endocyclic LiN bonds are stretched by 3−5 pm to 204 and 202 pm, respectively. Of the endocyclic angles only NLiN is affected; it decreases from 69.3° to 68.0°.

2.2.4. X-ray Structures of Dinuclear Lithium Amidinate Complexes [ArC(NSiMe$_3$)$_2$Li·D]$_2$. [4-FC$_6$H$_4$C(NSiMe$_3$)$_2$Li·OEt$_2$]$_2$ (**2c**) and [2,6-F$_2$C$_6$H$_3$C(NSiMe$_3$)$_2$Li·2,6-F$_2$C$_6$H$_3$CN]$_2$ (**3d**) belong to this type of complex. Details of their structure determination are listed in Table 2; Figure 3 shows their molecular structures. As discussed in section 2.2.1 possible structures for arylamidinate complexes of the composition [ArCN(SiMe$_3$)$_2$Li·D]$_2$ are the ladder structure **II** and the twisted structure **III** with **II′** as a possible intermediate. For **II** *cisoid* and *transoid* ladder-type arrangements are possible;[20] the structures reported in the literature exclusively show the *transoid* configuration, independent of the substituents.

Even [ferrocenyl-C(*N*-cyclohexyl)$_2$Li]$_2$ shows this arrangement.[14]

The most symmetric structure (C_i) was reported for [PhC(NPh)$_2$Li·OP(NMe)$_3$]$_2$.[11]

Alternatively to the ladder description this system might be considered as an eight-membered $C_2N_4Li_2$ heterocycle with two transannular NLi interactions. In all the reported structures this building principle is observed; the "transannular" bonds are significantly longer than the LiN bond lengths in the heterocycle. The average LiN bond distances (annular and transannular bonds) for the tridentate amidinate ligands in the three reported structures vary only within the range 209−212.6 pm.

(20) Downard, A.; Chivers, T. *Eur. J. Inorg. Chem.* **2001**, 2193−2201.

Table 3. Crystal Data and Structure Refinement for **4a**, **4e**, **5e**, and **6e**[a]

	4a	4e	5e	6e
empirical formula	$C_{20}H_{38}F_3LiN_4S\ i_2$	$C_{19}H_{34}F_5LiN_4Si_2$	$C_{21}H_{38}F_5LiN_2O_2Si_2$	$C_{21}H_{33}F_5LiN_2O_2Si_2$
fw	454.66	476.62	508.65	503.61
T/K	173(2)	173(2)	173(2)	173(2)
λ/Å	0.71073	0.71073	0.71073	0.71073
cryst syst	triclinic	triclinic	monoclinic	monoclinic
space group	$P\bar{1}$	$P\bar{1}$	$C2/c$	$P2_1/n$
a/Å	10.011(1)	9.745(2)	15.174(2)	13.254(3)
b/Å	10.644(1)	10.839(2)	13.383(2)	14.005(5)
c/Å	13.240(3)	14.008(3)	14.502(1)	14.929(5)
α/deg	90.78(1)	73.23(3)	90	90
β/deg	105.96(1)	71.45(3)	95.70(1)	92.27(2)
γ/deg	90.63(1)	87.39(3)	90	90
V/Å^3	1356.1(4)	1341.3(5)	2930.4(6)	2769.0(15)
Z	2	2	4	4
ρ_{calcd}/g cm^{-3}	1.113	1.180	1.153	1.208
μ(Mo Kα)/mm^{-1}	0.164	0.179	0.171	0.180
R1, wR2 [$I > 2\sigma(I)$]	0.0596, 0.1556	0.0514, 0.1427	0.0529, 0.1405	0.0680, 0.1807
R1, wR2 (all data)	0.0815, 0.1710	0.0729, 0.1521	0.0675, 0.1525	0.1225, 0.2045

[a] Details in common: Refinement method full-matrix least-squares on F^2; $\omega-2\theta$ scans; Siemens P4 diffractometer; $R1 = \sum||F_o| - |F_c||/\sum|F_o|$; $wR2 = \{\sum[w(F_o^2 - F_c^2)^2/\sum[w(F_o^2)^2]\}^{1/2}$; programs SHELX-97[29] and DIAMOND.[30]

Table 4. Crystal Data and Structure Refinement for **7e**, **8e**, and **10e**[a]

	7e	8e	10e
empirical formula	$C_{13}H_{19}F_5N_2Si_2$	$C_{10}H_{11}F_5N_2Si$	$C_{52}H_{72}F_{21}Li_5N_8Si_8$
fw	354.48	282.30	1467.60
T/K	213(2)	173(2) K	173(2)
λ/Å	0.71073	0.71073 pm	0.71073
cryst syst	triclinic	orthorhombic	monoclinic
space group	$P\bar{1}$	$Pna2_1$	$P2_1/c$
a/Å	6.244(1)	9.3309(18)	26.192(4)
b/Å	9.328(2)	16.322(2)	10.545(3)
c/Å	16.250(2)	17.059(5)	26.954(4)
α/deg	73.85(1)	90	90
β/deg	86.19(1)	90	99.330(10)
γ/deg	80.46(2)	90	90
V/Å^3	896.3(3)	2598.0(10)	7350(10)
Z	2	8	4
ρ_{calcd}/g cm^{-3}	1.313	1.443	1.327
μ(Mo Kα)/mm^{-1}	0.241	0.224	0.238
R1, wR2 [$I > 2\sigma(I)$]	0.0626, 0.1494	0.0495, 0.0994	0.0754, 0.1170
R1, wR2 (all data)	0.1007, 0.1695	0.0775, 0.1103	0.1876, 0.1516
absolute structure param		0.1(3)	

[a] Details in common: Refinement method full-matrix least-squares on F^2; $\omega-2\theta$ scans; Siemens P4 diffractometer; $R1 = \sum||F_o| - |F_c||/\sum|F_o|$; $wR2 = \{\sum[w(F_o^2 - F_c^2)^2/\sum[w(F_o^2)^2]\}^{1/2}$; programs SHELX-97[29] and DIAMOND.[30]

Scheme 3

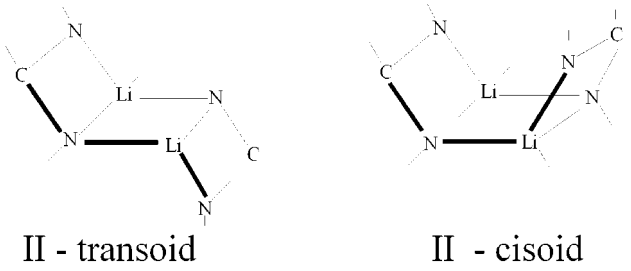

The twisted structure of type **III** is verified in **3d**; a very similar structure has been reported earlier by Eisen et al. for $[4\text{-}CH_3C_6H_4CN(SiMe_3)_2Li{\cdot}4\text{-}CH_3C_6H_4CN]_2$.[13] In **3d** one of the ligands symmetrically bridges (η^2) the two Li centers (LiN = 200.9 pm), while the other is bridging and bischelating (η^4) (LiN = 216.1 pm). A "ladder"-derived description for **III** seems not to be possible. Starting from an eight-membered $C_2N_4Li_2$ heterocycle, the structure of **3d** is easily formed by twisting one N−(Ar)C−N unit to an orthogonal

Scheme 4

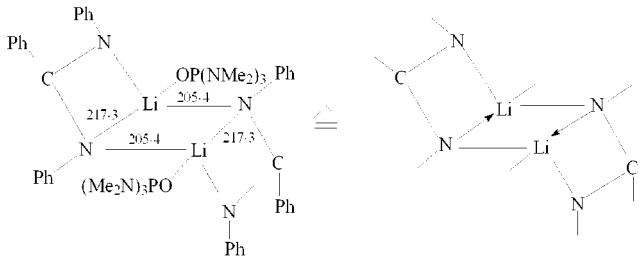

Scheme 5

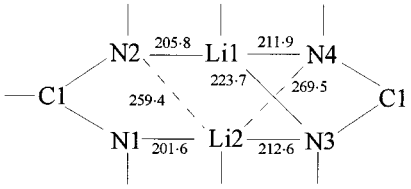

position until each of these nitrogens is symmetrically bridging the two Li centers. In the Eisen compound symmetrical bridging is not observed, but the average LiN bond distances for the biscoordinating and the quadruply coordinating amidinate ligands are exactly the same as in **3d** (200.5 and 216.5 pm, respectively).[13] The different coordination modes do not influence the bonding situation in the amidinate groups; for the bidentate and the tetradentate ligands average CN bond distances of 132.4 and 132.1 pm are determined. The NCN angle is however significantly influenced; N2C9N2 in the tetradentate amidinate group is appreciably smaller (118.8(4)°) than N1C1N1 in the bidentate group (123.5(4)°). Both aryl rings are oriented almost perpendicular to the corresponding NCN plane (89.9° at C1 and 85.3° at C14). Exactly the same average distances (132.5 and 132.8 pm) and angles (118.5(3)° and 123.6(3)°) were reported by Eisen et al. for the tolyl derivative.[13]

For **2c** we propose structure type **II′**, intermediate between **II** and **III**.

Since the bond distances N2Li2 (259.4(6) pm) and N4Li2 (269.5(6) pm) are very long, an alternative description of **2c** would be an eight-membered heterocycle with only one

Scheme 6

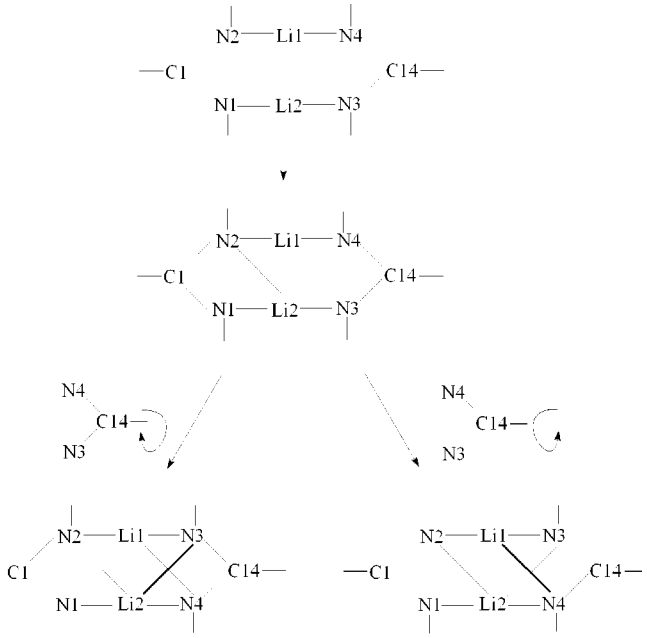

transannular bond. The coordination number of Li2 would be 3 instead of 5. In the previous discussion we derived from the reported structural data that for a bidentate amidinate ligand the average LiN distance is about 200 pm, for a tridentate ligand 209−212 pm, and for a tetradentate ligand 216−217 pm. For the ligand −N2−(Ar)C1−N1−, regarded as a tridentate ligand, the average LiN bond distance is far too long (222.3 pm); regarded as a doubly coordinating ligand, it is only slightly elongated (203.7 pm). Regarding the ligand −N4−(Ar)C14−N3−, tridentate bonding results in an average LiN bond distance of 216.1 pm, compared to that resulting from tetradentate bonding (226.9 pm); compared to the bond distances in compounds of type **II** it is too long.

Due to the weak interactions N2Li2 and N4Li2 the average LiN bond distances for the two ligands are slightly longer than expected for a doubly and triply coordinating ligand, respectively. The average CN distances in both different ligands are identical (132.8 and 132.5 pm, respectively). The N2C1N2 angle is 121.7(2)°, slightly smaller than found for the bidentate ligand in **3d**. The N4C14N3 angle (119.4(2)°) is larger than observed for the tetradentate ligand in **3d**. The LiN distances and the NCN angles support the view that **2c** might be regarded as the intermediate type **II′**.

2.2.5. X-ray Structures of Dinuclear Lithium Amidinate Complexes {[ArC(NSiMe$_3$)$_2$Li]$_2$·D}. The dinuclear amidinate complexes {[ArC(NSiMe$_3$)$_2$Li]$_2$D} (**2a**, **2b**, **2d**, and **2e**) represent a new type of structure. Details of the structure determinations are given in Table 2; the molecular structures are shown in Figure 4.

The geometries of the complexes are again best rationalized by starting from the eight-membered heterocycle $C_2N_4Li_2$. After the transannular Li2N2 bond is formed the fragment with N3 rotates either in front of or behind the plane of the paper (Scheme 6), resulting in the formation of two optical isomers. This twisting leads to additional

Scheme 7

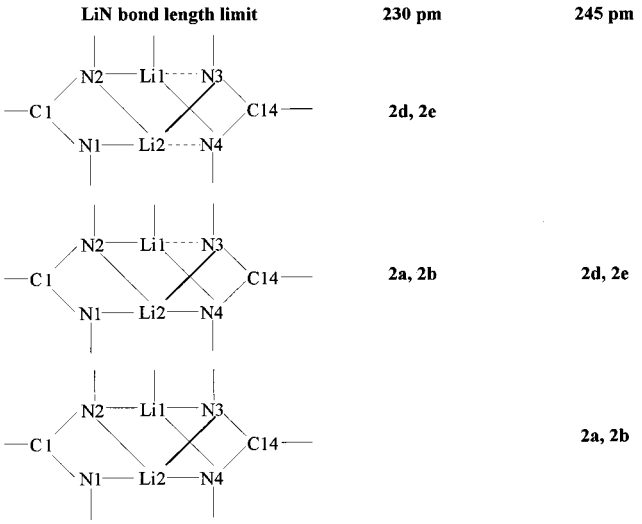

interactions N3Li1 and N4Li2, respectively, increasing the coordination numbers of Li1 and Li2 to 4, if NLi distances up to 255 pm are taken into consideration.

From the LiN bond length criterion the −N2−(Ar)C1−N2− fragment is clearly triply coordinating.

The average NLi bond length is 209 pm, similar to that found in compounds of type **II**. For the quadruply coordinating fragment −N4−(Ar)C14−N3− the average LiN distances vary between 221 and 225 pm, appreciably longer than those found in compounds of type **III** (216−217 pm). As discussed for **II′** this lengthening indicates the floating transition between weak interactions and "real" bond formation. Scheme 7 shows how the description of the bonding situation depends arbitrarily on the limits regarded as a "bond" for a LiN interaction (dashed lines indicate only weak interactions).

The average CN bond distances of the individual amidinate ligands in **2a**, **2b**, **2d**, and **2e** (132.0−133.0 pm) are not significantly dependent on the coordination mode; bonds to C1 seem to be slightly longer than those to C14. A distinct difference is found for the NCN angle. For the fragment N1C1N2 ("η^3", Scheme 1) this varies from 121.3° (**2a**) to 121.1° (**2b**) to 122.0° (**2d**) to 122.5° (**2e**), and for N3C14N4 ("η^4") from 118.3° (**2a**) to 119.5° (**2b**) to 120.1° (**2d**) to 120.9° (**2e**).

For **3d** we discussed (section 2.2.4) η^3 and η^4 coordination of the amidinate ligand with NCN angles of 123.6° and 118.8°, respectively. The decrease of the N1C1N2 angle and the increase of the N3C14N4 angle confirm the deviations from η^3 and η^4 coordination visualized in Scheme 7.

2.2.6. X-ray Structure of the Pentanuclear Fluoride-Centered Lithium Amidinate Complex {[C$_6$F$_5$C(NSiMe$_3$)$_2$Li]$_4$·LiF} (10e). Details of the structure determination of **10e** are given in Table 4. The molecular structure of the complex is shown in Figure 5a. In Figure 5b, the C_6F_5 substituents have been omitted for clarity.

While in recent years an appreciable number of cyclic systems have been reported as hosts for the halide ions Cl^-, Br^-, and I^-, for example,[21] those in which the fluoride ion acts as a guest are rather rare.[22] Recently we found that

perfluorocyclophosphazenes accept the "naked" fluoride; in $P_6N_6F_{13}^-$ a fluoride is the center of the anion, surrounded by a distorted octahedron of six phosphorus atoms.[23] **10e** represents the first example of an isolated molecule in which a fluoride interacts simultaneously with a trigonal bipyramid of five metals, which are incorporated into a macrocyclic cryptand (Figure 5b). Full lines represent bonds (LiN 199−213 pm) and dashed lines weak LiN transannular interactions (>250 pm). This macrocyclic cationic cryptand is formed from bridging the eight-membered $Li_2N_4C_2$ heterocycle at N8 and N3 by a nine-membered $Li_3N_4C_2$ chain. The distances from the central fluoride to the surrounding Li atom vary in the range 189(2)−197(2) pm; due to the high standard deviations they should be considered as not significantly different.

Alternatively the structure of **10e** can be discussed on the basis of the "laddering principle, a two-stage approach to describe lithium heterocarboxylates", very recently reviewed by Downard and Chivers.[20] According to the their terminology the dimerization product **II** (section 2.2.4) is formed by a "primary laddering process" from the monomeric units to give the primary laddering units (PLUs); interaction of these "PLUs" leads via a "secondary laddering process" to oligomeric (cages, chains) or polymeric species. This principle can also be applied to heteromolecular primary and secondary laddering. Chivers et al. reported the interaction of [*n*-BuC(N*t*Bu)$_2$Li]·2THF with LiX (X = OH, Cl, Br)[24] to give heteromolecular primary laddering units (HPLUs); these HPLUs dimerize in a secondary laddering process. In the formation of **10e** a HPLU from two monomers and LiF interacts with a twisted PLU, formed from two monomeric units, to give the observed complex **10e**.

Closely related to **10e** is the heterometallic complex {[PhC(NSiMe$_3$)$_2$Li]$_4$·MgO],[25] obtained in a reproducible 10−13% yield by Mulvey and co-workers among other unidentified products from the reaction of *n*,*sec*-Bu$_2$Mg, *n*-BuLi, 3(Me$_3$Si)$_2$NH, and 3PhCN in the presence of traces of oxygen. Instead of LiF the isoelectronic MgO unit is incorporated into the cage. Similar to **10e** a macrocyclic cryptand is formed from an eight-membered $Li_2C_2N_4$ heterocycle, bridged at opposite nitrogens by a nine-membered $Li_2C_2N_4Mg$ chain. The central oxide anion has trigonal bipyramidal geometry surrounded by four Li atoms and one Mg atom with the Mg atom in an equatorial position. In this trigonal bipyramid, in contrast to other trigonal bipyramidal species,[26] the axial LiO bonds are appreciably shorter than the equatorial LiO bonds. When Li_2O is used instead of MgO, the coordination number of the central oxygen increases to 6. The cage {[*n*-BuC(N*t*-Bu)$_2$ Li]$_4$·Li$_2$O}, where six Li atoms octahedrally surround a central oxide, was obtained by Chivers et al.[27] in a straightforward reaction from [*n*-BuC(N*t*-Bu)$_2$ Li] and LiOH; *n*-BuC[(N(H)*t*-Bu)](N*t*-Bu) is formed as a byproduct. Using the laddering terminology, the cage {[*n*-BuC(N*t*-Bu)$_2$Li]$_4$·Li$_2$O} is formed from two [Li-[*n*-BuC(N*t*-Bu)$_2$]$_2$ PLUs sandwiching the Li_2O in a secondary heteromolecular laddering step.

Scheme 8 [a]

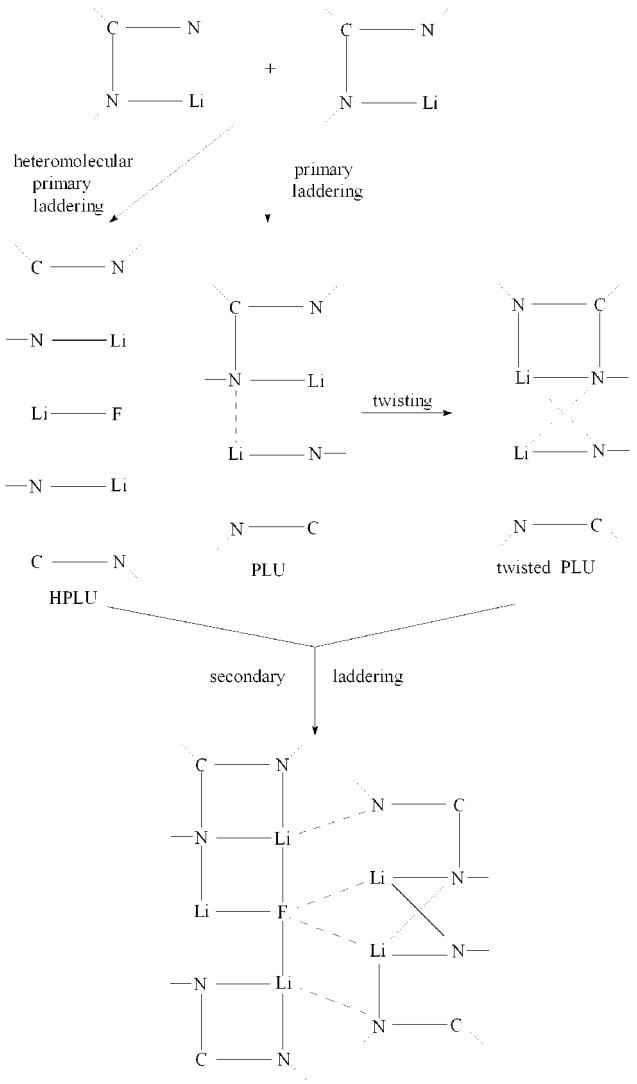

[a] Dashed lines characterize bonds formed during the laddering process.

Conclusions

Following the reported literature method,[8] new (Ar = 2-FC_6H_4, 4-FC_6H_4, 2,6-$F_2C_6H_3$) and previously described lithium fluoroarylamidinates (Ar = 4-$F_3CC_6H_4$,[8] C_6F_5[5,7]) were prepared and characterized by X-ray crystallography. Depending on the solvents used for these reactions and on the donor properties and concentration of coligands, structurally different types of products are obtained. The preparation of

(21) Schmidtchen, F. P.; Berger, M. *Chem. Rev.* **1997**, *97*, 1609−1646.
(22) Mews, R. *Inorganic Fluorine Chemistry Toward the 21st Century*; Thrasher J., Strauss, S., Eds.; ACS Symposium Series 555; American Chemical Society: Washington, DC, 1994; pp 148−166.
(23) Lork, E.; Böhler, D.; Mews, R. *Angew. Chem., Int. Ed. Engl.* **1995**, *34*, 2696−2698.
(24) Chivers, T.; Downard, A.; Parvez, M. *Inorg. Chem.* **1999**, *38*, 4347−4353.
(25) Kennedy, A. R.; Mulvey, R. E.; Rowlings, R. B. *J. Am. Chem. Soc.* **1998**, *120*, 7816−7824.
(26) Gillespie, R. J. *Molecular Geometry*; Van Nostrand Reinhold: London, 1972. Gillespie, R. J.; Popelier, P. L. A. *Chemical Bonding and Molecular Geometry*; Oxford University Press: New York, Oxford, 2001.
(27) Chivers, T.; Downard, A.; Yap, G. P. A. *J. Chem. Soc., Dalton Trans.* **1998**, 2603−2605.

the C_6F_5 derivative shows the complexity of this reaction, since different products are obtained depending on the reaction conditions used.[5−7] The lithium amidinates are very sensitive to moisture; the primary hydrolysis product $C_6F_5C(NSiMe_3)N(H)SiMe_3$ (**7e**) and the secondary hydrolysis product $C_6F_5C(NH)N(H)SiMe_3$ (**8e**) were isolated and structurally characterized. Following the method described by Oakley et al.[8] with Me_3SiCl, the lithium amidinates readily form persilylated arylamidines, $ArC(NSiMe_3)N(SiMe_3)_2$ (**9a**−**9d**), very useful reagents for the synthesis of heterocycles and coordination compounds. From the reaction with the pentafluorophenyl derivative a decomposition product, the fluorine-centered cage $\{[C_6F_5C(NSiMe_3)_2Li]_4\cdot LiF\}$ (**10e**), was isolated, where five Li atoms surround the fluorine in a trigonal bipyramidal arrangement. This is a further example of a reaction where metal halides or oxides act as templates in cage formation. Earlier Mulvey et al. reported the isoelectronic heterometallic Li/Mg complex $\{[C_6H_5C(NSiMe_3)_2Li]_4\cdot MgO\}$;[25] with Li_2O Chivers et al. characterized the oxygen-centered complex $\{[Li[n\text{-}BuC(Nt\text{-}Bu)_2]_4\cdot Li_2O\}$ in which octahedrally coordinated oxygen is surrounded by by six Li atoms.[24] Further investigations will show if these reaction principles can be generalized.

In the present paper further examples show the flexibility and versatility of the arylsilylamidinate ligands which give rise to a large number of different types of structures. In monomeric complexes $[ArC(NSiMe_3)_2Li\cdot 2D]$ the amidinate ligand acts in a bidentate chelating fashion; in the three different types of dinuclear complexes established $\eta^2-\eta^4$ coordination for the amidinate ligands is observed. Characteristic for the increasing denticity is the decrease of the NCN angle. This "angle criterion" is valid for di- and trinuclear species; it fails when heteroatoms are involved in cages (e.g., for **10e**).

A very helpful concept for the understanding of the structures of dimeric, oligomeric, and even cage structures such as those of **10e** is the "two-stage laddering principle" recently discussed in detail by Chivers and Downard.[20] The structures of the trimeric complexes such as $\{[PhC(NSiMe_3)_2Li]_3\cdot C_6H_5CN\}$[15] and the tolyl derivative[16] are also readily understood as insertion products of the fragments of $[ArC(NSiMe_3)_2Li\cdot C_6H_5CN]$ into a primary laddering unit, $[ArC(NSiMe_3)_2Li]_2$. An alternative to the laddering principle and a supplement for those cases where the laddering principle fails (and vice versa) starts from CNLi heterocycles as primary units followed by transannular bond formation and/or twisting of −N−(Ar)C−N− units with subsequent bond formation.

Experimental Section

Materials and Methods. All manipulations of air-sensitive materials were performed with the exclusion of oxygen and moisture under an inert atmosphere of dry nitrogen. Pentafluorobenzonitrile, 2-fluorobenzonitrile, 4-fluorobenzonitrile, 2,6-difluorobenzonitrile, TMEDA, and Me_3SiCl were commercial products, and used as received, except that TMEDA and Me_3SiCl were distilled and stored under nitrogen before use. The solvents were treated with CaH_2 and freshly distilled prior to use. $[4\text{-}F_3CC_6H_4C(NSiMe_3)_2Li]$[4] and $[(Me_3Si)_2NLi\cdot OEt_2]_2$[28] were prepared by published procedures. NMR spectra were recorded on Bruker DPX 200 (^1H, ^{19}F) and Bruker AM 360 NB (^{13}C, ^{29}Si) spectrometers in benzene-d_6. Chemical shifts are given with respect to Me_4Si (^1H, ^{13}C, ^{29}Si) and $CFCl_3$ (^{19}F). Infrared analyses were acquired as thin Kel-F and Nujol films using a Perkin-Elmer Paragon 500 FT-IR instrument. Melting points were obtained on a Gallenkamp melting point apparatus and are uncorrected.

Preparation of the Fluorinated Lithium *N,N′*-Bis(trimethylsilyl)benzamidinates 2a−2e. The fluorinated lithium *N,N′*-bis(trimethylsilyl)benzamidinates were prepared according to literature methods.[4] A 60 mmol sample of the benzonitrile **1a**−**1e** in 50 mL of diethyl ether was added dropwise to a stirred solution of 14.46 g (60 mmol) of lithium bis(trimethylsilyl)amide in 100 mL of diethyl ether at 0 °C, during which time a yellow to black solution was formed. After the solution was stirred at room temperature for 1 h, the solvent was removed under vacuum. The remaining solid was dissolved in as little *n*-hexane as possible and the solution filtered to remove undissolved impurities and cooled to −40 °C for several days to allow crystallization. The lithium *N,N′*-bis(trimethylsilyl)benzamidinates **2a**−**2e** were obtained as colorless or light yellow to brown crystalline solids, which should be stored in the cold.

$[(2\text{-}FC_6H_4C(NSiMe_3)_2Li)_2\cdot OEt_2]$ (2b). A 7.27 g (60 mmol) sample of 2-fluorobenzonitrile (**1b**) yields 13.00 g (20 mmol, 67%) of colorless crystals, mp 105 °C. Lithium *N,N′*-bis(trimethylsilyl)-2-fluorobenzamidinate contains 1/2 equiv of diethyl ether. ^1H NMR: δ 0.07 (s, 36H, $SiMe_3$), 1.07 (t, $^3J_{HH}$ = 7,0 Hz, 6H, CH_3), 3.33 (qa, $^3J_{HH}$ = 7.0 Hz, 4H, CH_2), 6.65−7.19 (m, 8H, C_6H_4F). ^{19}F NMR: δ −117.0 (s, 2F). $^{13}C\{^1H\}$ NMR: δ 2.0 (s, $SiMe_3$), 14.5 (s, CH_3), 66.3 (s, CH_2), 115.4 (d, $^2J_{CF}$ = 23 Hz, *m*-C_6FH_4), 123.3 (d, $^4J_{CF}$ = 3 Hz, C_6FH_4), 128.3 (d, $^3J_{CF}$ = 5 Hz, C_6FH_4), 128.4 (d, $^3J_{CF}$ = 7 Hz, C_6FH_4), 133.6 (d, $^2J_{CF}$ = 21 Hz, *ipso*-C_6FH_4), 157.9 (d, $^1J_{CF}$ = 243 Hz, *o*-C_6FH_4), 174.6 (s, NCN). $^{29}Si\{^1H\}$ NMR: δ −7.1 (s, $SiMe_3$). IR (cm^{-1}): 2951 m, 2896 m, 2260 w, 1665 w, 1611 m, 1575 w, 1488 vs, 1450 s, 1393 s, 1347 sh, 1278 w, 1243 s, 1221 s, 1156 w, 1098 m, 1066 w, 1029 w, 973 s, 938 w, 845 s, 757 s, 723 m, 674 m, 642 m, 620 w, 602 w, 554 m, 508 w.

$[4\text{-}FC_6H_4C(NSiMe_3)_2Li\cdot OEt_2]_2$ (2c). A 7.27 g (60 mmol) sample of 4-fluorobenzonitrile (**1c**) yields 11.2 g (15 mmol, 51%) of colorless crystals, mp 95 °C. Lithium *N,N′*-bis(trimethylsilyl)-4-fluorobenzamidinate contains 1 equiv of diethyl ether. ^1H NMR: δ 0.02 (s, 36H, $SiMe_3$), 1.05 (t, $^3J_{HH}$ = 7.0 Hz, 12H, CH_3), 3.29 (qa, $^3J_{HH}$ = 7.0 Hz, 8H, CH_2), 6.20−6.86 (m, 8H, C_6FH_4). ^{19}F NMR: δ −116.1 (s, 2F). $^{13}C\{^1H\}$ NMR: δ 3.9 (s, $SiMe_3$), 15.8 (s, CH_3), 66.3 (s, CH_2), 115.7 (d, $^2J_{CF}$ = 21 Hz, *m*-C_6FH_4), 128.2 (d, $^3J_{CF}$ = 7 Hz, *o*-C_6FH_4), 144.1 (d, $^4J_{CF}$ = 4 Hz, *ipso*-C_6FH_4), 163.1 (d, $^1J_{CF}$ = 245 Hz, *p*-C_6FH_4), 181.6 (s, NCN). $^{29}Si\{^1H\}$ NMR: δ −8.2 (s, $SiMe_3$). IR (cm^{-1}): 2952 m, 2895 m, 2254 w, 1890 w, 1681 w, 1603 m, 1502 sh, 1484 vs, 1383 s, 1243 s, 1189 w, 1154 w, 1122 w, 1093 w, 1069 w, 1002 w, 972 m, 936 w, 850 s, 754 s, 723 m, 678 w, 642 m, 620 m, 601 w, 548 w, 489 w.

$[(2,6\text{-}F_2C_6H_3C(NSiMe_3)_2Li)_2\cdot OEt_2]$ (2d). A 8.34 g (60 mmol) sample of 2,6-difluorobenzonitrile (**1d**) yields 11.09 g (16 mmol, 53%) of colorless to light brown crystals, mp 111 °C. Lithium *N,N′*-bis(trimethylsilyl)-2,6-difluorobenzamidinate contains 1/2 equiv of diethyl ether. ^1H NMR: δ 0.12 (s, 36H, $SiMe_3$), 1.09 (t, $^3J_{HH}$ = 7,1 Hz, 6H, CH_3), 3.32 (qa, $^3J_{HH}$ = 7.1 Hz, 4H, CH_2), 6.37−6.63 (m, 6H, $C_6H_3F_2$). ^{19}F NMR: δ −113.8 (s, 4F). $^{13}C\{^1H\}$ NMR: δ

(28) Lappert, M. F.; Slade, M. J.; Singh, A.; Atwood, J. L.; Rogers, R. D.; Shakir, R. *J. Am. Chem. Soc.* **1983**, *105*, 302−304.

1.7 (s, $SiMe_3$), 14.8 (s, CH_3), 66.1 (s, CH_2), 111.5 (dd, $^2J_{CF}$ = 24 Hz, $^4J_{CF}$ = 2 Hz, *m*-$C_6F_2H_3$), 123.0 (t, $^2J_{CF}$ = 27 Hz, *ipso*-$C_6F_2H_3$), 128.6 (t, $^3J_{CF}$ = 10 Hz, *p*-$C_6F_2H_3$), 158.7 (dd, $^1J_{CF}$ = 245 Hz, $^3J_{CF}$ = 9 Hz, *o*-$C_6F_2H_3$), 167,6 (s, NCN). $^{29}Si\{^1H\}$ NMR: δ −6.9 (s, $SiMe_3$). IR (cm^{-1}): 2945 m, 2894 m, 2266 m, 1619 s, 1583 m, 1562 m, 1547 w, 1494 s, 1480 vs, 1460 s, 1378 sh, 1363 s, 1311 w, 1296 m, 1252 s, 1230 m, 1156 w, 1124 w, 1016 s, 1003 sh, 997 sh, 979 m, 931 w, 887 m, 840 vs, 795 s, 764 sh, 746 s, 721 sh, 660 m, 607 m, 552 w, 521 m, 494 m, 480 sh.

[($F_5C_6C(NSiMe_3)_2Li)_2$·OEt_2] (2e). A 11.60 g (60 mmol) sample of pentafluorobenzonitrile (**1e**) yields 19.0 g (24 mmol, 73%) of yellow, under the microscope colorless, crystals, mp 97 °C. Lithium *N*,*N*′-bis(trimethylsilyl)pentafluorobenzamidinate contains 1/2 equiv of diethyl ether. ^1H NMR: δ 0.03 (s, 36H, $SiMe_3$), 1.02 (t, $^3J_{HH}$ = 7.0 Hz, 6H, CH_3), 3.23 (qa, $^3J_{HH}$ = 7.0 Hz, 4H, CH_2). ^{19}F NMR: δ −146.2 (m, 4F, *o*-F), −158.4 (t, $^3J_{FF}$ = 19.8 Hz, 2F, *p*-F), −164.7 (m, 4F, *m*-F). $^{13}C\{^1H\}$ NMR: δ 2.2 (s, $SiMe_3$), 15.2 (s, CH_3), 66.5 (s, CH_2), 120.8 (t, $^2J_{CF}$ = 23 Hz, *ipso*-C_6F_5), 139.0 (dm, $^1J_{CF}$ = 255 Hz, *o*-C_6F_5), 141.6 (dm, $^1J_{CF}$ = 254 Hz, *p*-C_6F_5), 143.1 (dm, $^1J_{CF}$ = 244 Hz, *m*-C_6F_5), 163.3 (s, NCN). $^{29}Si\{^1H\}$ NMR: δ −4.3 (s, $SiMe_3$). IR (cm^{-1}): 2948 m, 2888 m, 2786 sh, 1674 m, 1647 m, 1617 sh, 1522 sh, 1500 vs, 1400 s, 1340 s, 1283 m, 1246 s, 1184 w, 1150 w, 1108 s, 1061 m, 987 s, 946 w, 840 s, 768 m, 749 s, 725 s, 674 m, 638 m, 585 w, 544 m.

[2,6-$F_2C_6H_3C(NSiMe_3)_2Li$·2,6-$F_2C_6H_3CN]_2$ (3d). A 6.96 g (50 mmol) sample of 2,6-difluorobenzonitrile (**1d**) in 50 mL of diethyl ether was added dropwise to a stirred solution of 6.03 g (25 mmol) of lithium bis(trimethylsilyl)amide in 50 mL of diethyl ether at 0 °C, during which time a yellow to black solution was formed. After the solution was stirred at room temperature for 1 h, the solvent was removed under vacuum. The remaining solid was dissolved in the smallest amount of *n*-hexane as possible and the solution filtered to remove undissolved impurities and cooled to −40 °C for several days to allow crystallization, mp 115 °C. A 7.20 g (8 mmol, 64% yield) sample of colorless to light brown crystals was obtained. ^1H NMR: δ 0.23 (s, 36H, $SiMe_3$), 5.90−6.63 (m, 12H, $C_6H_3F_2$). ^{19}F NMR: δ −104.4 (s, 4F), −113.7 (s, 4F). $^{13}C\{^1H\}$ NMR: δ 2.7 (s, $SiMe_3$), 92.5 (t, $^2J_{CF}$ = 19 Hz, *ipso*- $C_6F_2H_3$), 110.7 (s, NC), 112.3 (dd, $^2J_{CF}$ = 19 Hz, $^4J_{CF}$ = 6 Hz, *m*-$C_6F_2H_3$), 112.8 (dd, $^2J_{CF}$ = 19 Hz, $^4J_{CF}$ = 4 Hz, *m*-$C_6F_2H_3$), 124.6 (t, $^2J_{CF}$ = 27 Hz, *ipso*-$C_6F_2H_3$), 127.9 (t, $^3J_{CF}$ = 9 Hz, *p*-$C_6F_2H_3$), 137.0 (t, $^3J_{CF}$ = 10 Hz, *p*-$C_6F_2H_3$), 159.8 (dd, $^1J_{CF}$ = 245 Hz, $^3J_{CF}$ = 9 Hz, *o*-$C_6F_2H_3$),), 164.3 (dd, $^1J_{CF}$ = 262 Hz, $^3J_{CF}$ = 4 Hz, *o*-$C_6F_2H_3$), 168.0 (s, NCN). $^{29}Si\{^1H\}$ NMR: δ −7.4 (s, $SiMe_3$). IR (cm^{-1}): 2950 m, 2895 m, 2262 m, 1674 m, 1619 m, 1583 m, 1503 s, 1460 vs, 1409 w, 1378 s, 1294 w, 1273 w, 1242 s, 1158 w, 1022 w, 1003 m, 974 m, 842 s, 793 m, 762 m, 740 m, 718 w, 676 w, 656 w, 604 m, 521 w.

Preparation of the TMEDA Complexes 4a and 4e of Fluorinated Lithium *N*,*N*′-Bis(trimethylsilyl)benzamidinates. The lithium *N*,*N*′-bis(trimethylsilyl)benzamidinates were dissolved in a small amount of toluene, and twice the volume of TMEDA was added. After the solution was stirred for 30 min at room temperature, the solvent and excess TMEDA were removed under vacuum. Colorless and temperature- and moisture-sensitive crystals were obtained after recrystallization of the residue in a little *n*-hexane at −40 °C.

[4-$F_3CC_6H_4C(NSiMe_3)_2Li$·TMEDA] (4a). A 8.50 g (11 mmol) sample of **2a** yields 8.21 g (18 mmol, 82%) of colorless, temperature-sensitive crystals, mp 110 °C. ^1H NMR: δ −0.06 (s, 18H, $SiMe_3$), 1.71 (s, 4H, CH_2), 1.91 (s, 12H, CH_3), 7.12 (d, $^3J_{HH}$ = 8.1 Hz, 2H,C_6H_4), 7.31 (d, $^3J_{HH}$ = 8.1 Hz, 2H, C_6H_4). ^{19}F NMR: δ −62.8 (s, 3F, CF_3). $^{13}C\{^1H\}$ NMR: δ 4.2 (s, $SiMe_3$), 46.4 (s, CH_3), 57.3 (s, CH_2), 125.8 (qa, $^3J_{CF}$ = 4 Hz, *m*-C_6H_4,), 126.3 (qa, $^1J_{CF}$ = 272 Hz, CF_3,), 127.5 (s, *o*-C_6H_4), 129.1 (qa, $^2J_{CF}$ = 32 Hz, *p*-C_6H_4), 152.4 (s, *ipso*-C_6H_4), 178.3 (s, NCN). $^{29}Si\{^1H\}$ NMR: δ −11.9 (s, $SiMe_3$). IR (cm^{-1}): 2954 s, 2873 m, 2836 m, 2793 m, 1922 w, 1850 w, 1784 m, 1660 m, 1613 m, 1478 vs, 1410 s, 1324 s, 1292 m, 1240 s, 1166 s, 1130 s, 1104 w, 1064 m, 1040 w, 1021 m, 984 w, 945 w, 860 s, 831 s, 752 m, 670 m, 630 w, 617 w, 556 m.

[$C_6F_5C(NSiMe_3)_2Li$)·TMEDA] (4e). A 9.95 g (12.5 mmol) sample of **2e** yields 7.62 g (16 mmol, 64%) of colorless, temperature-sensitive crystals, mp 95 °C. ^1H NMR: δ −0.05 (s, 18H, $SiMe_3$), 1.71 (s, 4H, CH_2), 1.86 (s, 12H, CH_3). ^{19}F NMR: δ −143.5 (dddd, $^3J_{FF}$ = −26.0 Hz, $^4J_{FF}$ = −3.2 Hz, $^4J_{FF}$ = −1.2 Hz, $^5J_{FF}$ = 9.1 Hz, 2F, *o*-F), −161.1 (tt, $^3J_{FF}$ = −21.2, $^4J_{FF}$ = −1.2, 1F, *p*-F), −164.3 (dddd, $^3J_{FF}$ = −21.2 Hz, $^3J_{FF}$ = −26.0 Hz, $^4J_{FF}$ = −2.7 Hz, $^5J_{FF}$ = 9.1 Hz, 2F, *m*-F). $^{13}C\{^1H\}$ NMR: δ 2.9 (s, $SiMe_3$), 46.5 (s, CH_3), 57.7 (s, CH_2), 122.5 (t, $^2J_{CF}$ = 29 Hz, *ipso*-C_6F_5), 138.9 (dm, $^1J_{CF}$ = 252 Hz, *o*-C_6F_5), 140.9 (dm, $^1J_{CF}$ = 251 Hz, *p*-C_6F_5), 143.0 (dm, $^1J_{CF}$ = 242 Hz, *m*-C_6F_5), 159.6 (s, NCN). $^{29}Si\{^1H\}$ NMR: δ −11.3 (s, $SiMe_3$). IR (cm^{-1}): 2955 s, 2874 m, 2837 m, 2797 m, 1677 w, 1646 m, 1514 vs, 1467 s, 1391 s, 1291 m, 1242 s, 1181 w, 1158 w, 1130 w, 1107 m, 1064 w, 1036 w, 1021 w, 985 s, 946 m, 834 vs, 790 w, 771 w, 747 m, 676 m, 641 m, 584 m, 553 m, 502 w.

Preparation of [$C_6F_5C(NSiMe_3)_2Li$·2OEt_2] (5e). A 7.5 g (9.4 mmol) sample of **2e** was dissolved in 20 mL of diethyl ether with stirring. Large colorless crystals formed on storage at −40 °C (6.3 g, 12.3 mmol, 65% yield), mp 47 °C. ^1H NMR: δ 0.00 (s, 18H, $SiMe_3$), 0.98 (t, $^3J_{HH}$ = 7.0 Hz, 12H, CH_3), 3.20 (qa, $^3J_{HH}$ = 7.0 Hz, 8H, CH_2). ^{19}F NMR: δ −143.6 (s, 2F, *o*-F), −159.5 (s, 1F, *p*-F), −163.6 (s, 2F, *m*-F). $^{13}C\{^1H\}$ NMR: δ 2.6 (s, $SiMe_3$), 15.6 (s, CH_3), 66.4 (s, CH_2), 122.0 (t, $^2J_{CF}$ = 29 Hz, *ipso*-C_6F_5), 138.9 (dm, $^1J_{CF}$ = 254 Hz, *o*-C_6F_5), 141.1 (dm, $^1J_{CF}$ = 250 Hz, *p*-C_6F_5), 143.2 (dm, $^1J_{CF}$ = 242 Hz, *m*-C_6F_5), 160.6 (s, NCN). $^{29}Si\{^1H\}$ NMR: δ −9.8 (s, $SiMe_3$). IR (cm^{-1}): 2956 m, 2899 m, 1676 w, 1648 m, 1507 vs, 1450 m, 1391 s, 1289 w, 1244 s, 1187 w, 1154 w, 1108 s, 1068 m, 985 s, 847 vs, 770 w, 749 s, 732 m, 676 m, 640 w, 601 w, 584 w, 531 m, 500 w, 472 w.

Preparation of [$C_6F_5C(NSiMe_3)_2Li$·2THF] (6e). A 7.5 g (9.4 mmol) sample of **2e** was dissolved in 50 mL of tetrahydrofuran with stirring. The volatiles were removed under vacuum, and the oily residue was dissolved in approximately 20 mL of *n*-hexane. On storage of the yellow solution at −40 °C, light yellow, under the microscope colorless, crystals were formed (8.1 g, 16 mmol, 85% yield), mp 78 °C. ^1H NMR: δ −0.01 (s, 18H, $SiMe_3$), 1.32 (m, 4H, β-CH_2), 3.57 (m, 4H, α-CH_2). ^{19}F NMR: δ −142.9 (s, 2F, *o*-F), −158.9 (s, 1F, *p*-F), −163.3 (s, 2F, *m*-F). $^{13}C\{^1H\}$ NMR: δ 2.4 (s, $SiMe_3$), 26.3 (s, CH_2), 69.3 (s, OCH_2), 121.5 (t, $^2J_{CF}$ = 34 Hz, *ipso*-C_6F_5), 138.9 (dm, $^1J_{CF}$ = 254 Hz, *o*-C_6F_5), 141.4 (dm, $^1J_{CF}$ = 254 Hz, *p*-C_6F_5), 143.3 (dm, $^1J_{CF}$ = 244 Hz, *m*-C_6F_5), 161.5 (s, NCN). $^{29}Si\{^1H\}$ NMR: δ −8.2 (s, $SiMe_3$). IR (cm^{-1}): 2959 m, 2896 m, 1677 m, 1649 w, 1516 vs, 1492 vs, 1398 s, 1362 m, 1245 s, 1107 s, 1051 m, 986 s, 838 vs, 768 w, 750 m, 725 m, 672 w, 643 w, 601 w, 584 w.

Preparation of $C_6F_5C(NSiMe_3)N(H)SiMe_3$ (7e). A 0.32 mL (0.32 g, 17.8 mmol) sample of water was added via a syringe to a solution of 7.1 g (8.9 mmol) of **2e** in 50 mL of *n*-hexane. The precipitate of lithium hydroxide was removed by filtration through a thin layer of Celite and washed with a small amount of *n*-hexane, and the solution was then reduced to around 20 mL under vacuum. On storage at −40 °C, colorless crystals were obtained (3.9 g, 11 mmol, 62% yield), mp 48 °C. ^1H NMR: δ −0.07 (s, 9H, $SiMe_3$), 0.21 (s, 9H, $SiMe_3$), 3.86 (s, 1H, NH), ^{19}F NMR: δ −144.3 (m, 2F, *o*-F), −156.7 (t, $^3J_{FF}$ = −21.2 Hz, 1F, *p*-F), −162.7 (m, 2F, *m*-F). $^{13}C\{^1H\}$ NMR: δ 0.5 (s, $SiMe_3$), 0.9 (s, $SiMe_3$), 116.6 (t,

$^2J_{CF}$ = 24 Hz, *ipso*-C_6F_5), 138.6 (dm, $^1J_{CF}$ = 255 Hz, *o*-C_6F_5), 142.1 (dm, $^1J_{CF}$ = 254 Hz, *p*-C_6F_5), 143.7 (dm, $^1J_{CF}$ = 241 Hz, *m*-C_6F_5), 146.8 (s, NCN). $^{29}Si\{^1H\}$ NMR: δ −5.5 (s, $SiMe_3$), 4.9 (s, $SiMe_3$). IR (cm^{-1}): 3425 m, 3335 w, 2960 s, 2902 m, 1677 s, 1652 sh, 1518 s, 1496 vs, 1402 vs, 1309 m, 1250 s, 1212 m, 1134 w, 1107 m, 990 s, 929 w, 839 vs, 766 m, 748 m, 722 w, 636 m, 581 w, 539 m, 480 m.

Preparation of $C_6F_5C(NH)N(H)SiMe_3$ (8e). A 0.48 mL (0.48 g, 26.7 mmol) sample of water was added via a syringe to a solution of 7.1 g (8.9 mmol) of **2e** in 50 mL of *n*-hexane. The precipitate of lithium hydroxide was removed by filtration through a thin layer of Celite and washed with a small amount of *n*-hexane, and the solution was then reduced to around 20 mL under vacuum. On storage at −40 °C, colorless crystals were obtained (3.0 g, 10.6 mmol, 60% yield), mp 49 °C. ^1H NMR: δ 0.06 (s, 9H, $SiMe_3$), 3.87 (s, 1H, NH), ^{19}F NMR: δ −144,2 (m, 2F, *o*-F), −156.6 (t, $^3J_{FF}$ = −21.1, 1F, *p*-F), −162.6 (m, 2F, *m*-F). $^{13}C\{^1H\}$ NMR: δ −0.4 (s, $SiMe_3$), 115.6 (t, $^2J_{CF}$ = 25 Hz, *ipso*-C_6F_5), 137.4 (dm, $^1J_{CF}$ = 252 Hz, *o*-C_6F_5), 140.9 (dm, $^1J_{CF}$ = 259 Hz, *p*-C_6F_5), 142.5 (dm, $^1J_{CF}$ = 246 Hz, *m*-C_6F_5), 146.3 (s, NCN). $^{29}Si\{^1H\}$ NMR: δ −5.5 (s, $SiMe_3$). IR (cm^{-1}) 3421 m, 3357 w, 2961 m, 2902 w, 1667 s, 1652 sh, 1625 m, 1519 s, 1499 s, 1450 m, 1399 s, 1363 w, 1309 w, 1251 s, 1212 m, 1157 sh, 1134 m, 1107 s, 1054 w, 991 s, 929 w, 865 sh, 841 s, 759 s, 748 s, 722 m, 699 sh, 636 m, 608 w, 581 w, 539 m, 479 m.

Preparation of Fluorinated *N,N,N′*-Tris(trimethylsilyl)benzamidinates 9b−9d. A 60 mmol sample of benzonitrile in 50 mL of diethyl ether was added dropwise to 14.46 g (60 mmol) of lithium bis(trimethylsilyl)amide in 100 mL of diethyl ether at 0 °C with stirring, during which time a yellow to black solution was formed. The solvent was pumped off after the solution was stirred for 1 h at ambient temperature. The remaining black residue was dissolved in 100 mL of toluene and 7.6 mL (6.53 g, 60 mmol) of Me_3SiCl added via a syringe. After 5 h of reflux the precipitated LiCl was filtered through a thin layer of Celite and the solvent removed in vacuo. The residue was fractionally distilled in an oil-pump vacuum using a short air-cooler. The products were thus obtained as pale yellow liquids or low-melting-point solids.

2-$FC_6H_4C(NSiMe_3)[N(SiMe_3)_2]$ (9b). A 7.27 g (60 mmol) sample of 2-fluorobenzonitrile (**1b**) yields 16.57 g (47 mmol, 78%) of pale yellow solid, mp 42 °C. ^1H NMR: δ 0.13 (s, 27H, $SiMe_3$), 6.21−7.04 (m, 4H, C_6H_4F). ^{19}F NMR: δ −114.8 (dt, $^3J_{FH}$ = 9.3 Hz, $^4J_{FH}$ = 6.0 Hz, 1F). $^{13}C\{^1H\}$ NMR: δ 2.4 (s, $SiMe_3$), 115.6 (d, $^2J_{CF}$ = 22 Hz, *m*-C_6FH_4), 123.4 (d, J_{CF} = 4 Hz, C_6FH_4), 129.6 (d, J_{CF} = 4 Hz, C_6FH_4), 130.0 (d, J_{CF} = 7 Hz, C_6FH_4), 131.1 (d, $^2J_{CF}$ = 17 Hz, *ipso*-C_6FH_4), 158.9 (d, $^1J_{CF}$ = 247 Hz, *o*-C_6FH_4), 161.3 (s, NCN). $^{29}Si\{^1H\}$ NMR: δ −0.1 (s, $SiMe_3$). IR (cm^{-1}): 3421 w, 2958 s, 2901 m, 1650 s, 1635 vs, 1613 s, 1578 w, 1495 sh, 1487 m, 1453 s, 1398 m, 1362 w, 1296 m, 1247 vs, 1217 m, 1154 w, 1133 m, 1093 m, 941 w, 920 w, 845 vs, 759 vs, 688 m, 632 w, 616 w, 552 w, 527 w, 491 w.

4-$FC_6H_4C(NSiMe_3)[N(SiMe_3)_2]$ (9c). A 7.27 g (60 mmol) sample of 4-fluorobenzonitrile (**1c**) yields 14.05 g (38 mmol, 63%) of a pale yellow solid, mp 45 °C. ^1H NMR: δ 0.08 (s, 27H, $SiMe_3$), 6.93−7.36 (m, 4H, C_6H_4F). ^{19}F NMR: δ −112.9 (tt, $^3J_{FH}$ = 8.6 Hz, $^4J_{FH}$ = 5.5 Hz, 1F). $^{13}C\{^1H\}$ NMR: δ 2.5 (s, $SiMe_3$), 114.6 (d, $^2J_{CF}$ = 21 Hz, *m*-C_6FH_4), 130.0 (d, $^3J_{CF}$ = 7 Hz, *o*-C_6FH_4), 139.8 (d, $^4J_{CF}$ = 3 Hz, *ipso*-C_6FH_4), 163.0 (d, $^1J_{CF}$ = 249 Hz, *p*-C_6FH_4), 167.4 (s, NCN). $^{29}Si\{^1H\}$ NMR: δ −10.4 (s, $SiMe_3$). IR (cm^{-1}): 3048 w, 2958 s, 2901 s, 1936 w, 1902 w, 1632 vs, 1602 s, 1506 s, 1403 m, 1377 m, 1290 m, 1248 vs, 1154 m, 1121 s, 1090 m, 994 s, 943 w, 883 s, 848 vs, 756 s, 676 s, 642 w, 622 w, 595 m, 518 m.

2,6-$F_2C_6H_3C(NSiMe_3)[N(SiMe_3)_2]$ (9d). A 8.34 g (60 mmol) sample of 2,6-difluorobenzonitrile (**1d**) yields 10.27 g (28 mmol, 46%) of a pale yellow liquid. ^1H NMR: δ 0.13 (s, 27H, $SiMe_3$), 6.27−6.63 (m, 3H, $C_6H_3F_2$). ^{19}F NMR: δ −113.3 (t, $^3J_{FH}$ = 7 Hz, 2F). $^{13}C\{^1H\}$ NMR: δ 2.2 (s, $SiMe_3$), 111.2 (dd, $^2J_{CF}$ = 19 Hz, $^4J_{CF}$ = 7 Hz, *m*-$C_6F_2H_3$), 120.3 (t, $^2J_{CF}$ = 23 Hz, *ipso*-$C_6F_2H_3$), 129.5 (t, $^3J_{CF}$ = 10 Hz, *p*-$C_6F_2H_3$), 154.7 (s, NCN), 159.3 (dd, $^1J_{CF}$ = 245 Hz, $^3J_{CF}$ = 8 Hz, *o*-$C_6F_2H_3$). $^{29}Si\{^1H\}$ NMR: δ 7.3 (s, $SiMe_3$). IR (film, cm^{-1}): 3421 w, 2957 s, 2900 m, 1636 s, 1586 s, 1555 w, 1466 s, 1406 m, 1281 vs, 1249 vs, 1234 sh, 1186 w, 1137 s, 1061 w, 1003 s, 934 sh, 877 sh, 839 vs, 789 m, 756 s, 743 s, 673 s, 639 w, 622 w, 588 m, 517 m, 494 w.

Preparation of $\{[C_6F_5C(NSiMe_3)_2Li]_4LiF\}$ (10e). A 6.3 mL (5.43 g, 50 mmol) sample of Me_3SiCl in 15 mL of toluene was added to a solution of 19.90 g (25.0 mmol) of **2e** in 130 mL of toluene. After 1 h under reflux the precipitate of lithium chloride was removed by filtration through a thin layer of Celite and the volatiles were removed under vacuum. From a solution of the dark red oil in C_6D_6 after several weeks of storage at 6 °C, colorless crystals were obtained.

Crystallographic Analysis. The single-crystal X-ray structure determinations (Tables 1−4) were carried out on a Siemens P4 diffractometer or on a Stoe IPDS (**3d**, **4e**) using Mo Kα (0.71073 Å) radiation with a graphite monochromator. Details of the data collection and refinement are given in Tables 1−4. Refinement was based on F^2; R1 = $\sum||F_o| - |F_c||/\sum|F_o|$, and wR2 = $\{\sum[w(F_o^2 - F_c^2)^2/\sum[w(F_o^2)^2]\}^{1/2}$. The programs SHELX-97[29] and DIAMOND[30] were used. The structures were solved by direct methods (SHELXS).[29] Subsequent least-squares refinement (SHELXL 97-2)[29] located the positions of the remaining atoms in the electron density maps. Non-hydrogen atoms were refined anisotropically. Hydrogen atoms bonded to nitrogen atoms were located from the electron density map. All other hydrogen atoms were placed in calculated positions using a riding mode and refined isotropically in blocks.[31]

The crystals were mounted using KEL-F oil onto a thin glass fiber.

The following results were obtained: (**2b**) The fluorine atom on the second phenyl ring is disordered over two sites. (**2c**) The ethyl groups in the diethyl ether on Li1 are disordered over two sites. (**2d**) The ethyl groups in the diethyl ether on Li1 and the methyl groups on Si3 are disordered over two sites. (**2e**) The ethyl groups in the diethyl ether on Li1 are disordered over two sites. (**4a**) The methylene groups of the TMEDA molecule are disordered over two sites. (**4e**) One methylene group of the TMEDA molecule is disordered over two sites. (**6e**) The THF molecules are partly disordered over two sites.

Acknowledgment. Financial support by the FNK, University of Bremen, is gratefully acknowledged.

Supporting Information Available: This material is available free of charge via the Internet at http://pubs.acs.org.

IC011099T

(29) Sheldrick, G. M. *SHELX-97*; University of Göttingen: Göttingen, Germany, 1997.
(30) *DIAMOND-Visual Crystal Structure Information System*; Crystal Impact: Bonn, Germany.
(31) Crystallographic data (excluding structure factors) for the structures in this paper have been deposited with the Cambridge Crystallographic Data Centre as supplementary publication nos. CCDC 161840 (**10e**), 161841 (**7e**), 161842 (**2a**), 161843 (**2d**), 161844 (**5e**), 161845 (**2e**), 161846 (**4e**), 161847 (**4a**), 161848 (**6e**), 161849 (**2c**), 161850 (**3d**), 161851 (**8e**), and 172609 (**2b**). Copies of the data can be obtained, free of charge, on application to CCDC, 12 Union Rd., Cambridge CB2 1EZ, U.K. (fax +44 1223 336033 or e-mail deposit@ccdc.cam.ac.uk).